BNWL-1481
UC-80

[redacted]

CRITICAL EXPERIMENTS IN AN MTR MOCKUP USING PHOENIX FUEL

E. C. Davis, Jr.
R. I. Smith
L. D. Williams

June 1970

[redacted]

AEC RESEARCH & DEVELOPMENT REPORT

BNWL-1481

BATTELLE NORTHWEST
BATTELLE MEMORIAL INSTITUTE PACIFIC NORTHWEST LABORATORIES
3000 STEVENS DRIVE, P. O. BOX 999, RICHLAND, WASHINGTON 99352

LEGAL NOTICE

PACIFIC NORTHWEST LABORATORY
RICHLAND, WASHINGTON
operated by
BATTELLE MEMORIAL INSTITUTE
for the
UNITED STATES ATOMIC ENERGY COMMISSION UNDER CONTRACT AT(45-1)-1830

AEC-RL RICHLAND, WASH.

BNWL-1481
UC-80,
Reactor Technology

CRITICAL EXPERIMENTS IN AN MTR MOCKUP USING PHOENIX FUEL

E. C. Davis, Jr.
R. L. Smith
L. D. Williams

Reactor Physics Department
Physics and Engineering Division

June 1970

BATTELLE MEMORIAL INSTITUTE
PACIFIC NORTHWEST LABORATORIES
RICHLAND, WASHINGTON 99352

Printed in the United States of America
Available from
National Technical Information Service
National Bureau of Standards, U.S. Department of Commerce
Springfield, Virginia 22151
Price: Printed Copy $3.00; Microfiche $0.65

BNWL-1481

CRITICAL EXPERIMENTS IN AN MTR MOCKUP USING PHOENIX FUEL

E. C. Davis, Jr.
R. I. Smith
L. D. Williams

ABSTRACT

Utilization of ^{240}Pu as a convertible poison in plutonium-fueled systems is being studied under the Phoenix Fuel Reactor Program at Pacific Northwest Laboratory (PNL). An extensive experimental program using Phoenix fuel in a critical mockup of the Materials Testing Reactor (MTR) has been completed in the Plutonium Recycle Critical Facility[1] (PRCF) at PNL. The PRCF-Phoenix mockup duplicated as closely as possible the physical configuration of the MTR in order to determine the characteristics of such a core. The experiments performed in this mockup provided information on the reactivity effects and power distributions to be expected of an MTR-Phoenix fuel core prior to the loading of a full core in the MTR. These data have provided an excellent test of the computational methods currently being applied to Phoenix Fuel cores. The results of the PRCF experiments are presented in this report.

TABLE OF CONTENTS

LIST OF FIGURES

LIST OF TABLES

CRITICAL EXPERIMENTS IN AN MTR MOCKUP USING PHOENIX FUEL

E. C. Davis, Jr.
R. I. Smith
L. D. Williams

I. INTRODUCTION

Utilization of ^{240}Pu as a convertible poison in plutonium-fueled systems is being studied at Pacific Northwest Laboratory (PNL). These studies are being made under the auspices of the Phoenix Fuel Reactor Program, a research and development project concerned with the use of plutonium fuel that contains a relatively high percentage of the isotope ^{240}Pu for extending reactivity lifetime characteristics. The idea of employing suitable plutonium isotope composites to improve time-dependent reactivity performance of certain reactor types was originated at Hanford Laboratories (now PNL) around 1958.

A possible application for Phoenix fuel is the replacement of ^{235}U fuel cores in research reactors.[2] In addition to extending lifetimes, Phoenix fuel offers the potential for increased neutron flux for the same power density. This potential could be important to research reactors. Computational studies have been made [3,4] that show the potential inherent in the utilization of ^{240}Pu as a convertible poison. The conversion of the fertile ^{240}Pu into the fissionable ^{241}Pu helps balance the loss of the initial ^{239}Pu during power operation. Thus, a plutonium-fueled system could be developed using ^{240}Pu as a reactivity control in the same way that boron is used as the burnable poison in ^{235}U fueled systems. The ^{240}Pu has the added advantages of conversion to a fissionable isotope ^{241}Pu,

as well as having cross sections more compatible with those of the fissile material.[5] An important feature of this concept is the "rebirth" of the fissile ^{241}Pu isotope from the ^{240}Pu "ashes". It was because of the analogy of this effect to that of the legendary "Phoenix Bird" of ancient Egyptian mythology, that it was dubbed "Phoenix Effect." The fuel composites required to produce a "Phoenix Effect" became known as "Phoenix Fuels."

As a demonstration of the Phoenix principle, a burnup experiment was planned and executed for the Materials Testing Reactor (MTR) utilizing a complete core of Phoenix Fuel. The MTR is a light-water moderated, beryllium-reflected, high-flux test reactor operated by Idaho Nuclear Corporation (INC) at the National Reactor Testing Station near Idaho Falls. The possibility of using the MTR as a Phoenix fuel test bed was proposed in the early summer of 1966, and a 3 x 9 full plutonium loading with 8 control rods in the core was designated as the configuration.

To answer the many questions associated with a complete new core loading using Phoenix fuel, a series of critical experiments were conducted at PNL. These critical experiments were conducted in the Physical Constants Testing Reactor (PCTR), Critical Approach Facility (CAF), and Plutonium Recycle Critical Facility[1] (PRCF), prior to the loading of a full core in the MTR. Data from the PCTR and CAF experiments were used in studying the conceptual neutronic characteristics of Phoenix-fueled cores, and to test and improve on methods used to predict the neutronic behavior of unirradiated Phoenix cores. These experiments have been previously reported.[6,7] The final results of the PRCF experiments are presented in this report. Preliminary results have been previously documented, and these reports are listed under Reference 8.

A critical mockup of the MTR-Phoenix fuel core was constructed for use in the PRCF, and an extensive experimental program has been carried out to determine the characteristics of such a core. This mockup duplicated as closely as possible the physical configuration planned for the MTR experiment. The experimental program conducted in this facility has assisted in determining the reliability of the calculational models in the areas of localized flux and power peaking, control system strength, and neutron leakage effects. The results of these analytical studies are currently being documented[9].

II. SUMMARY AND CONCLUSIONS

An extensive experimental program has been conducted to determine the characteristics of Phoenix fuel with various core loadings in the MTR mockup. Among the measurements made were the following:

- Shim-free critical size.
- Full core critical banked shim height.
- Power distributions for various configurations.
- Shim rod reactivity worths.
- Simulated regulating rod reactivity worth.
- Temperature coefficients of reactivity.
- Void reactivity worths.
- Fuel plate reactivity worths.
- Kinetics parameters.

These measurements are described in detail in this report.

Initial critical loading for the PRCF-Phoenix core was achieved with 16-1/2 stationary fuel assemblies in a 3 × 5-1/2 array (as shown in Section V, Figure 7). The stationary boxes in core locations X and Z-2, 4 and 6 were relocated to other fixed element positions in order to allow insertion of the shims. The eight shim rod-fuel follower assemblies were then installed and the remainder of the 3 × 9 core was loaded. An approach-to-critical experiment was performed by banked withdrawal of the shims and the critical array for this core configuration was achieved with the shims withdrawn to 65%.

The core was then unloaded and removed from the PRCF cell to permit restacking of the beryllium reflector in the region

---

* *For purposes of this report, a shorthand form of notation has been adopted which indicates shim positions by stating that they were located in both* X *and* Z-2, 4, 6 *and* 8 *instead of* X-2, X-4, X-6, X-8, Z-2, Z-4, Z-6, *and* Z-8.

adjacent to the core tank wall. This was required in order to improve the similarity between the PRCF core and the planned MTR-Phoenix core. The beryllium volume fraction in this region was increased from about 70% to nearly 94%, with a corresponding reduction in the volume of H_2O.

After restacking the beryllium at the core-reflector interface, a new shim-free critical loading was achieved with 14-1/4 fuel boxes arranged in a 3 × 4-3/4 box array (as shown in Section V, Figure 7). The new critical mass was about 5.6 kg of plutonium, as compared with the critical mass of 6.5 kg of plutonium before restacking. The full-core configuration of 19 stationary fuel elements and 8 shims was implemented by adding the remaining fixed boxes and shims after relocating the elements that were in X and Z-4, and 6. This full-core loading in the PRCF achieved criticality with the shims withdrawn to 59% as compared with 65% withdrawn prior to restacking of the beryllium. To simulate xenon poisoning in this core, borated polyethylene sheeting was attached to the plates of the fixed fuel elements. Distribution of this plastic throughout the core produced a shim-critical height of 62.8% withdrawn, or an equivalent poisoning effect of 15 mk in worth.

The experimental program was terminated after a special core loading was constructed to obtain data from a configuration more amenable to calculation. This core configuration consisted of a shim rod without the fuel follower being placed in location Y-1 and followed by the loading about it of a symmetric array of 15-5/8 stationary fuel elements to obtain criticality.

The flux and power distribution measurements made within the shims and fixed boxes as well as in the reflector region of the PRCF-Phoenix core were designed to provide information on the relative shapes and magnitudes of the power profiles. Thus, the experiments in the MTR-Phoenix Fuel mockup not only included

critical size measurements, but power distribution measurements as well. These distributions were used to extrapolate the conditions expected at initial startup in the normally shimmed MTR-Phoenix Fuel Core. An additional extrapolation was also made with the measured data obtained from the poisoned, shimmed core. Special attention was paid to the power peaking observed at the core boundaries. The power peaking at the bottom edge of the fuel cores was also investigated as part of this study. It was determined that by tapering the fuel plate cores, the power peak at that location was essentially eliminated. In addition, gold and copper cadmium ratios were measured in the special core loading which consisted of the cadmium shim rod located in position Y-1.

Other measurements made in the PRCF-Phoenix core have provided information on the worth of fuel follower shim control rods, temperature and void coefficients of reactivity as well as reactivity changes upon loss of fuel plates. Additional reactivity measurements were made to determine the worth of a simulated MTR regulating rod. The measured data obtained for the determination of the shim rod strength and temperature coefficients of the PRCF-Phoenix core have been analyzed and the results of least square fits to these data are presented. This report also includes experiments that were conducted to measure the control and shut-down capability as well as the kinetics parameters of the PRCF-Phoenix core.

The measurements in the MTR mockup have helped to define the specifications for fabrication of fuel plates for the MTR Experiment[10] and have provided the data needed for a good first-order estimate of the power levels which could be safely attained during the operation of the MTR. The kinetics parameters and reactivity coefficient measurements have provided data which were essential to the safety analysis of the MTR Experiment.[11] In addition, these data have provided an

excellent test of the computational methods currently being applied to Phoenix Fuel cores. The use of the PRCF-Phoenix mockup experiment changed the role of the calculations to a tool for the conversion of these experimental results to the predicted MTR conditions. In summary, these measurements have provided information on the reactivity effects and power distributions to be expected of a Phoenix fuel core in the MTR and have proved to be valuable in helping to plan[12] the burnup experiment. Without the measurements to assist in the MTR-Experiment design, severe limitations on the power would have resulted because of power peaking at the bottom edge of the core.

III. GEOMETRICAL ARRANGEMENT

A top-plane view of the critical mockup of the MTR-Phoenix fuel core that was operated in the PRCF is shown in Figure 1. This core consisted of a 3 × 9 array of plate-type fuel elements similar in design to the standard MTR fuel elements. Cross sections of this core showing the two different side views are illustrated in Figures 2 and 3. A side view of the core is shown in Figure 2 with the shim assemblies and stationary fuel assemblies located in the even and odd columns, respectively. The notation "bank" or "banked" is used in this report to indicate that the shims are level at the same percent withdrawn. Columns 2 and 4 in Figure 2 illustrate the positions of the shim assemblies when withdrawn to 0 and 100%, respectively; whereas, the shim assemblies in columns 6 and 8 are withdrawn approximately 60%. The cadmium section of the shim assembly had a stroke of 30-3/4 inches. This required that the cadmium section be withdrawn 6 inches before the top of the fuel follower was positioned equal to the bottom of the stationary fuel.

These assemblies were loaded into the core lattice structure in the PRCF cell by designating which particular row (X, Y or Z) and column (1 through 9) they were to occupy. The eight shim control rods with fuel followers containing 12 plates each were* inserted into the even-numbered columns of both rows X and Z. The remaining core locations were designed to accomodate the 19 stationary fuel elements that contained 16 plates each. The dimensional details of the shim fuel followers and stationary fuel elements are given in Table I. The fuel within these assemblies was comprised of A1-19.95 wt% Pu. The nominal

---

* *For purposes of this report, a shorthand form of notation has been adopted which indicates shim positions by stating that they were located in both X and 2-2, 4, 6 and 8 instead of* X-2, *X-4, X-6,* X-8, *2-2, Z-4, Z-6, and Z-8.*

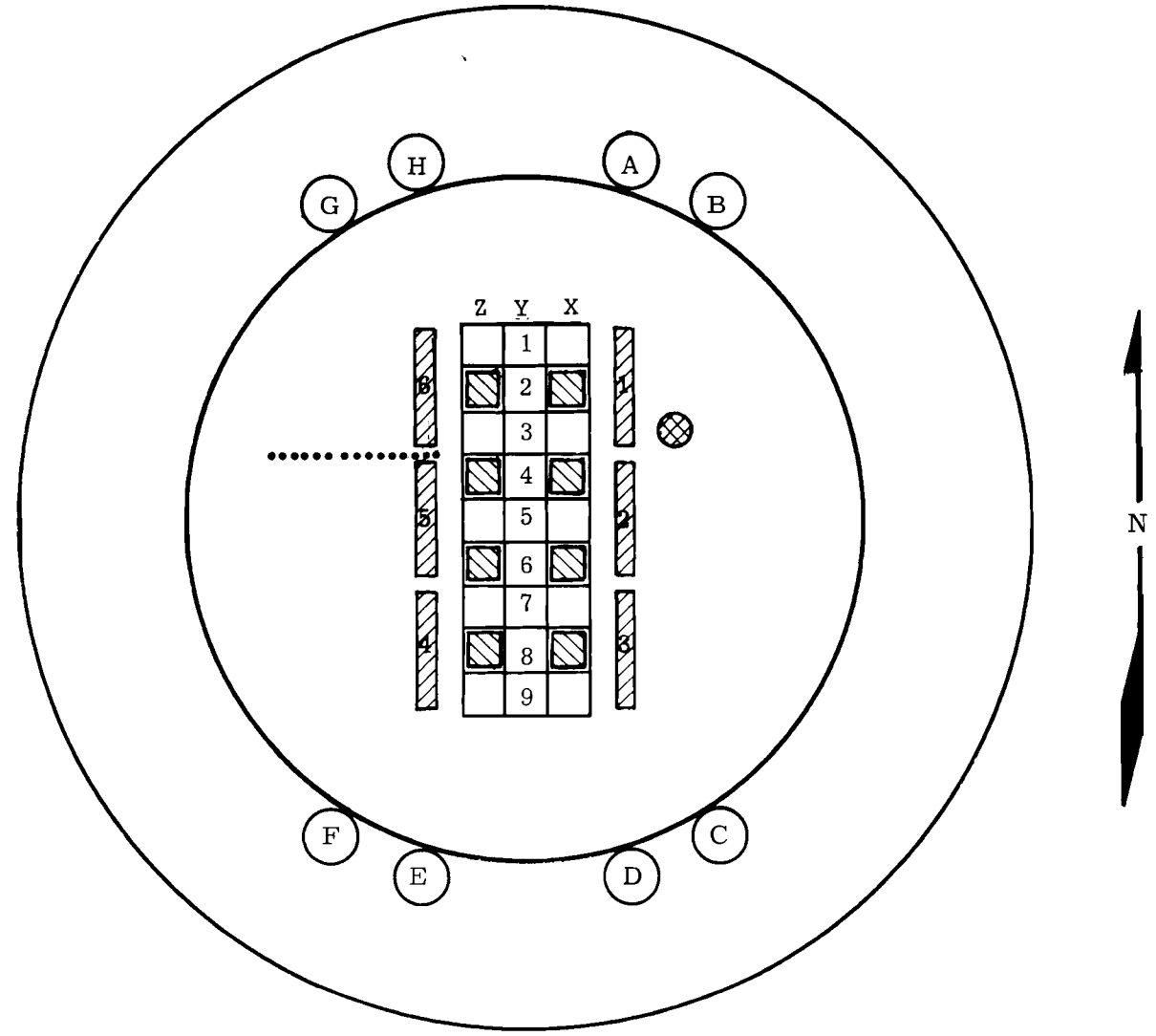

16 PLATE FUEL ELEMENT

12 PLATE SHIM-FOLLOWER ASSEMBLY

SAFETY SHEET THIMBLES

15 VERTICAL SLOTS FOR PIN ACTIVATION

REMOVABLE BERYLLIUM LOG (HOLE NUMBER 1)

(A) LINEAR CHANNEL NUMBER 2

(B) LOG CHANNEL NUMBER 1

(D) STARTUP CHANNEL (SCALER)

(E) LOG CHANNEL NUMBER 2

(F) LINEAR CHANNEL NUMBER 1

(G) STARTUP CHANNEL (LCRM)

FIGURE 1. PRCF–Phoenix Core Configuration, Top View

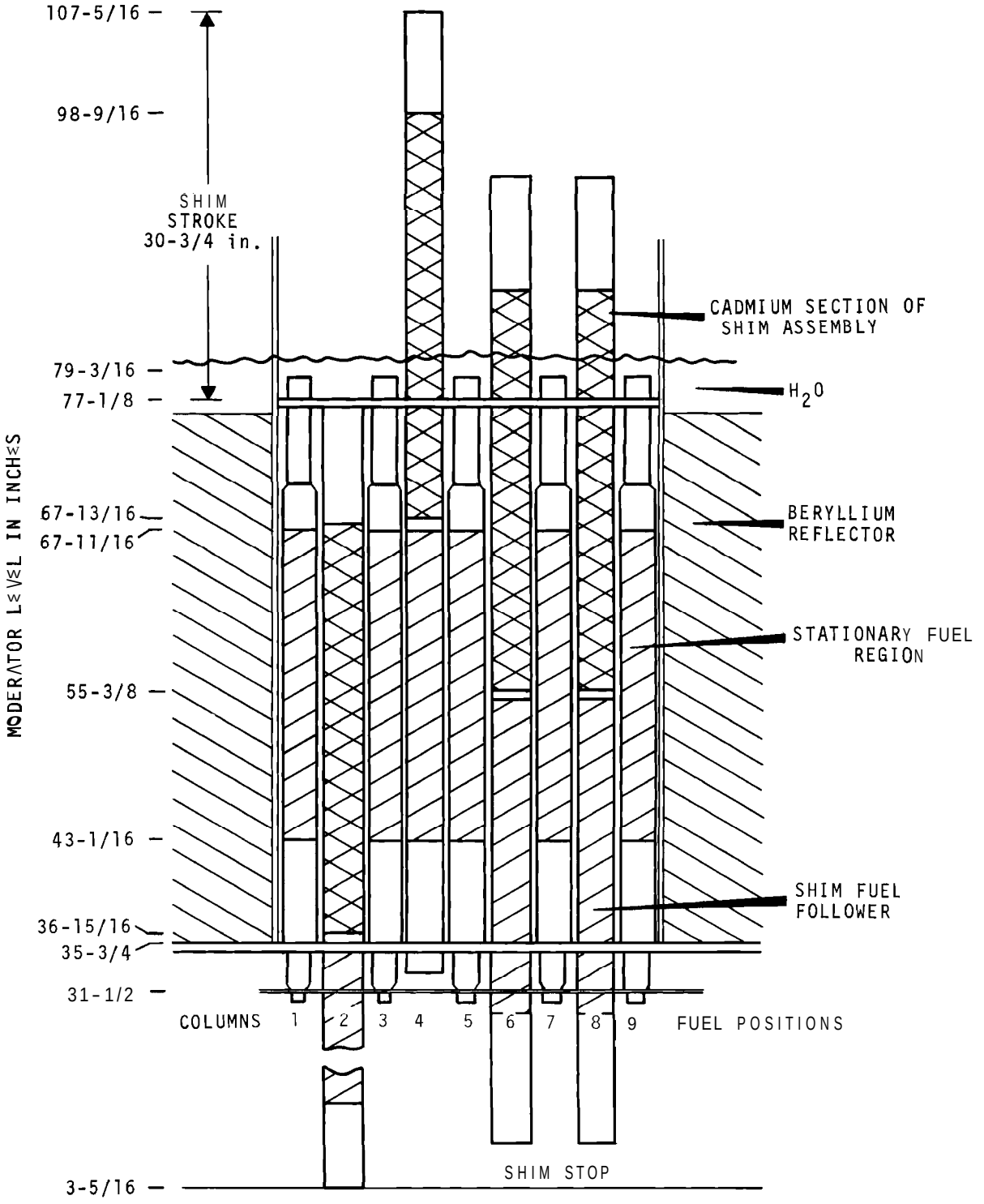

FIGURE 2. PRCF–Phoenix Core Configuration, Side View

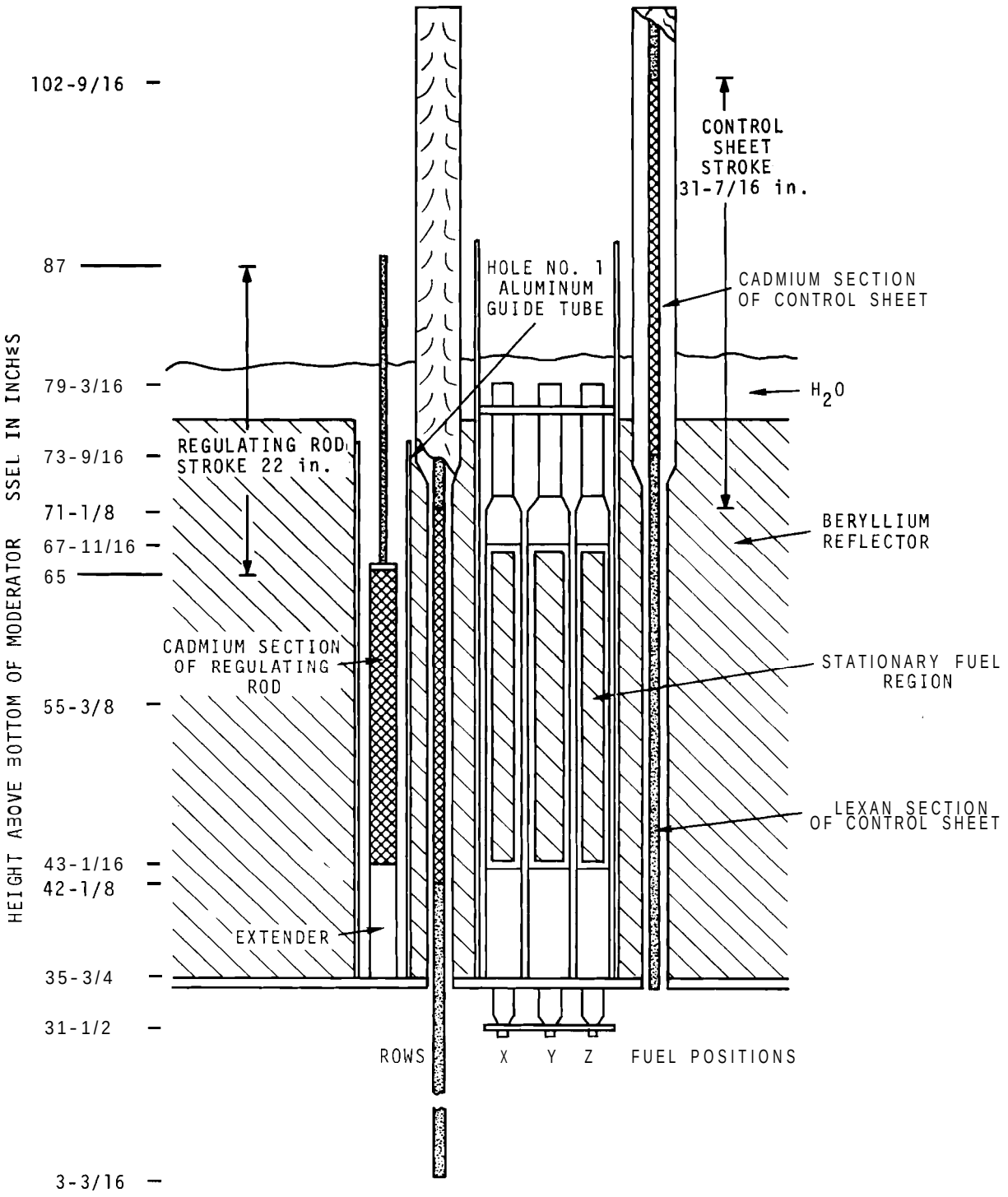

FIGURE 3. PRCF-Phoenix Core Configuration, End View Showing the Mockup of the MTR-Regulating Rod

TABLE I. PRCF–Phoenix Fuel Element Details

	Stationary	Shim Follower
Number of Fuel Elements	19	8
Number of Fuel Plates per Element	16	12
Dimensions (in inches) of Fuel Element. Assembly	3.169 × 2.996 × 24.625	3.068 × 2.835 × 24.625
Dimensions (in inches) of Fuel Plate Assembly	0.08 × 2.84 × 24.625	0.08 × 2.679 × 24.625
Dimensions (in inches) of Fuel Core	0.04 × 2.52 × 23.5	0.04 × 2.355 × 23.5
Dimensions (in inches) of Coolant Channel	0.118 × 2.65 × 23.5	0.118 × 2.370 × 23.5

isotopic composition of the plutonium in this fuel was: 76.92% ^{239}Pu, 19.31% ^{240}Pu, 3.18% ^{241}Pu, and 0.59% ^{242}Pu. A disassembled view of a stationary element used in this Phoenix experiment is shown at the top of Figure 4. The top and bottom end boxes are shown relative to the fuel plates in this assembly. The aluminum side plate has been removed to obtain a better view of the internal array of 16 plates. The bottom view is of a typical Phoenix Fuel Shim Rod. The side plate has been removed to show the 12-plate array in the fuel follower.

The MTR critical mockup was beryllium-reflected and light-water moderated. The radial reflector consisted of beryllium logs and triflutes which had been wrapped with polyethylene tubing. The safety sheets shown in Figures 1 and 3 were constructed of rectangular sheets of 0.030-inch thick cadmium encased in Lexan. These sheets had a stroke of 31-7/16 inches and they served as the primary control mechanism for reactor operation in irradiation studies and approaches to asymptotic periods.

FIGURE 4. PRCF – Phoenix Core. Shim Rod with Fuel Follower and Stationary or Fixed Assembly

Nuclear instrumentation provided the necessary data for operating this reactor and was also used in conjunction with the safety circuit for reactor scrams in the event of an off-normal condition. These instruments consisted of six chambers located at the periphery of the beryllium reflector (as shown in Figure 1) using either fission chambers or neutron-sensitive ion chambers as detectors. These included two startup channels (Scaler and LCRM in D and G), two intermediate range channels (Log N-1 and 2 in B and E), and two high level safety channels (Linear 1 and 2 in F and A).

IV. REACTOR OPERATION AND CONTROL

The safety sheets located in the beryllium reflector (shown in Figures 1 and 3) served as the primary control mechanism for reactor operation in irradiation studies and approaches to asymptotic periods. The initial operational procedure used for reactor startup at this facility consisted of dropping the moderator through a dump valve to a storage tank located below the PRCF reactor tank. Three of the safety sheets would then be withdrawn to their full "out" position. These sheets were armed by the safety circuit so they would automatically insert in order to provide rapid shutdown reactivity if it was needed. Scram of the safety circuit would interrupt power to the magnets that restrained the sheets in place. This power interruption would cause the safety sheets to drop. Cell entry would then be made to set the shims individually by hand or to make fuel element modifications as needed to record a period measurement in the range of 2 to 36¢ reactivity. After completing the required core-loading change and locking the shims out so they could not be moved up or down, the reactor cell would be sealed and only then would the moderator be pumped back into the reactor tank. The moderator level was controlled by setting an adjustable weir mechanism to the height required for that measurement. All of the remaining safety sheets would then be fully withdrawn individually to initiate the multiplication needed for observing and recording of period measurements.

A loss of reactivity from the PRCF core at the rate of 2¢/hr. was encountered during the preliminary measurements. This phenomenon was originally believed to be caused by formation of small hydrogen bubbles from an aluminum-water reaction on the surfaces in the core which produced voids in the moderator.

To inhibit the bubble formation, all the fuel assemblies were boiled in H_2O for 6 to 8 hours to improve the aluminum oxide film on the surfaces of these assemblies. Subsequent reactivity measurements showed that the problem had not been completely eliminated but had been reduced in magnitude, and a series of exploratory measurements were initiated to isolate the cause. It was noted that by driving the sheets full-in (instead of dropping them), this effect on the reactor was further mini.-mized, and the reproducibility of period measurements was improved.

There were also indications that part of the reactivity losses might be caused by small changes in the temperature of the H_2O coolant that occurred during the experiment. Temperature measurements were performed as part of the exploratory measurements, and these measurements were found to be extremely sensitive to the time that the H_2O was left in the reactor tank following the periods of heating. This was believed to be caused by cooling on the uninsulated top and bottom reflector surfaces. Measurements made immediately following moderator mixing displayed consistent results, and this procedure was incorporated as a standard technique for reactor operations.

The reactivity worths of the safety sheets were measured initially in the 16-1/2 element clean core and in the first 3 × 9 shimmed core loaded into the PRCF. After restacking the beryllium reflector, the reactivity worths of the safety sheets were again measured in the shim-free core containing 14-1/4 stationary fuel boxes and in the second 3 × 9 shimmed core.

The worths were determined by comparing the rate of flux decay following a sheet drop to that calculated for various step changes in reactivity. The subsequent results show that there appeared to be a small interaction between the safety sheets since the measured worth of all sheets was slightly less than

the sum of the measured worths of the individual sheets. The results of the sheet measurements for the various core configurations are tabulated in Table II.

TABLE II. Sheet Reactivity Worth Measurements in PRCF–Phoenix Fuel Cores

	Original		Restacked Reflector	
	Shim-free 16-1/2 Boxes	Shimmed 27 Boxes	Shim-free 14-1/4 Boxes	Shimmed 27 Boxes
Total System	15 mk	14 mk	21 mk	19-1/2 mk
Strongest Sheet	5 mk	3-1/2 mk	7-1/4 mk	4-1/2 mk

The worths of the safety sheets were increased about 40 to 45% due to the improvement in beryllium density between the core tank wall and the sheet locations in the shim-free cores. Increases of 40% and 30%, respectively, were observed for the total package and strongest sheet, as compared to the previous 3 × 9 shimmed core.

V. ACTIVITY MEASUREMENTS AT THE PRCF

Flux and power distribution measurements were made as part of the experimental program conducted with this type of fuel in various core configurations. The power profiles were measured by gamma scanning the fission product activities produced within the cores of the Phoenix fuel plates after an irradiation in the PRCF. These irradiated plates were scanned by utilizing the gamma scanning facility at the PRCF. The flux profiles were determined by measuring the activity obtained from pure copper pin detectors. These detectors were 0.25 inches in length and 0.035 inches in diameter, and they were distributed throughout the reactor fuel core and beryllium reflector. The activity measurements were obtained in order to determine the shape of the power profiles within the stationary fuel elements and the fuel followers of the shim rods as well as the magnitude of power peaking at the fuel edges.

A block diagram of the gamma scanning circuit at the PRCF is shown in Figure 5. The two-channel circuit gave decay-corrected data by using the preset count mode. The gross fission product activities in the plates with energies greater than approximately 0.3 MeV were measured using a NaI detector. The spatial resolution was defined by a steel collimator whose length was 11 inches and whose aperture was decreased from 0.25 × 0.52 inches to 0.128 × 0.52 inches. The decrease in the aperture was required to increase the resolution of the measured power distributions. This modification was completed before measurements were obtained from the second 3 × 9 full core. The relative position of this collimator to that of the detector and fuel plate is shown in Figure 6.

A typical irradiation in the PRCF consisted of operating the reactor for 30 minutes at a power of 100 watts. Plate scanning would be initiated about 2 hours after shutdown.

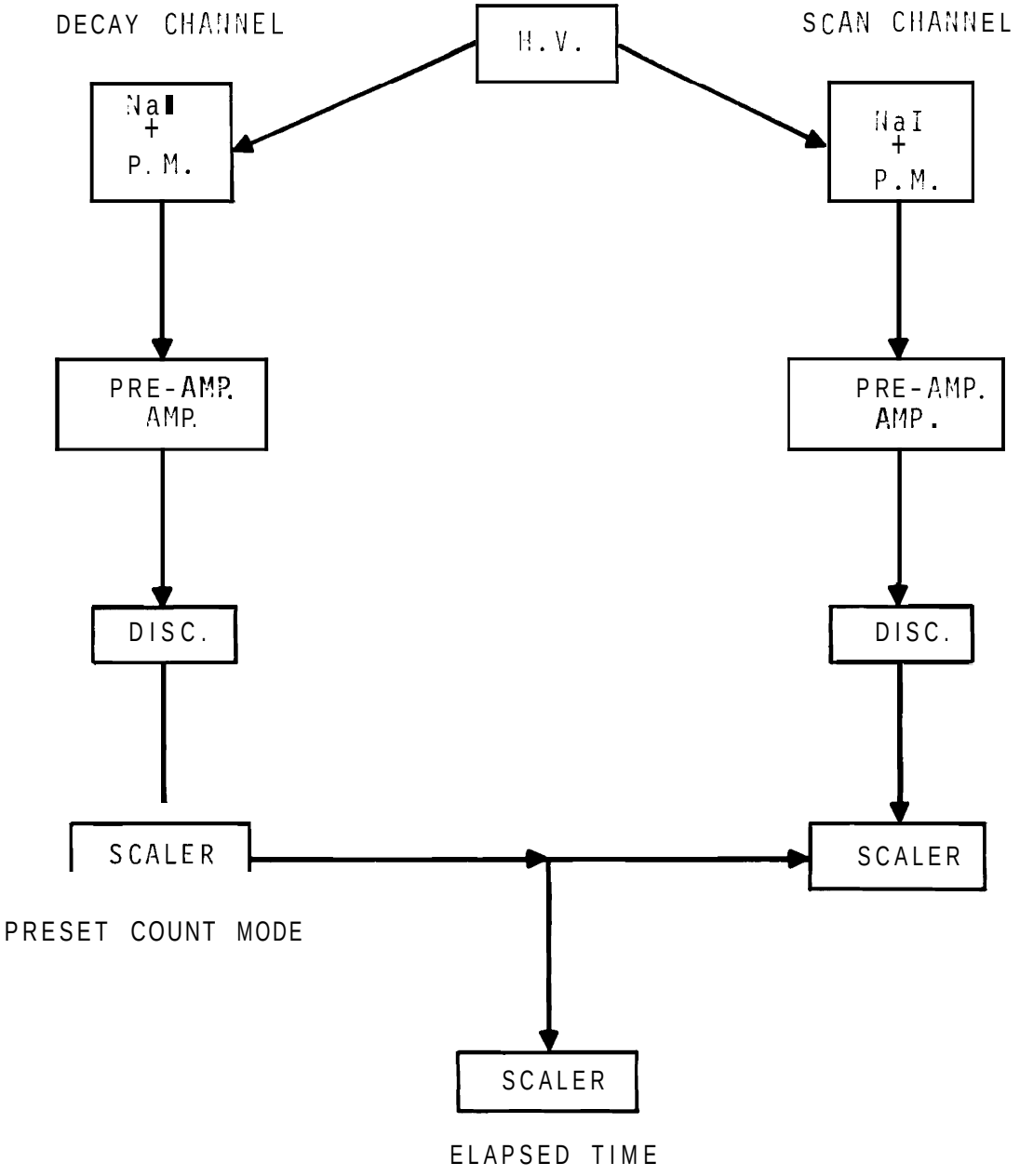

FIGURE 5. Block Diagram of the Two-Channel Circuit Used to Gamma Scan PRCF-Phoenix Fuel Plates

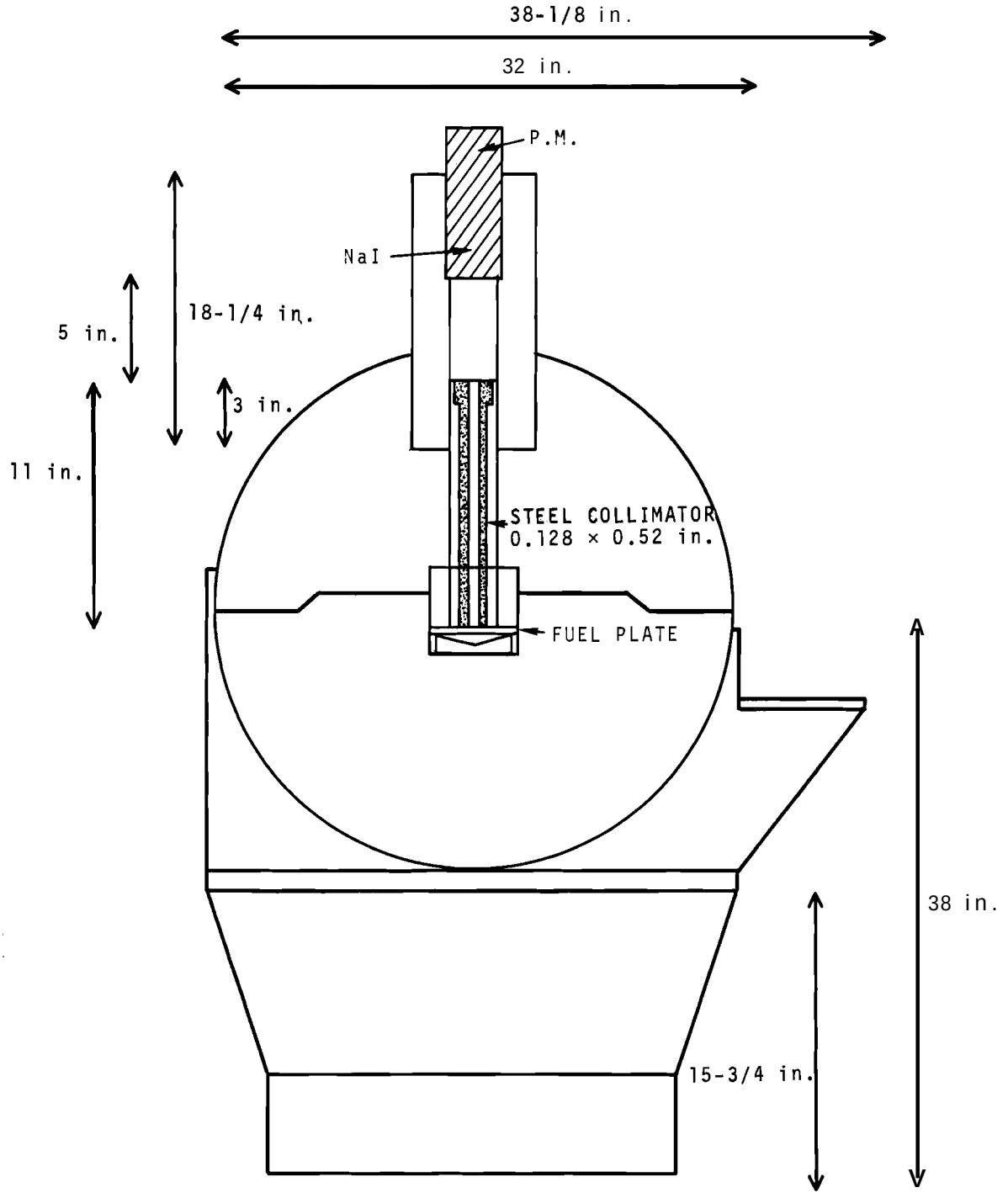

FIGURE 6. Centerline View of Scanning Cask at the PRCF–Gamma Scanning Facility

Background counting rates were recorded on both the decay and scan channels. A plate adjacent to those that were selected to be counted was then inserted into the decay correcting portion of the two-channel circuit. Throughout the course of a y-scanning measurement, a standard plate would be intermittently counted at the position of peak flux to allow for a drift correction to be applied to the data recorded on the scan channel. A scan of the regular fuel plate would be obtained by counting and moving this plate in predetermined increments until the counting time grew too large. The preset count would then be reduced and the above stepwise procedure was continued until the scheduled plate scans were completed. This reduction in the preset count would occur at time intervals of 2 to 2-1/2 hours. Immediately before and after this reduction in the preset count value was made, the output observed for the background and standard plates were recorded to determine the normalization factor needed to correct the scans for the variations in the preset count rate. After the final counts were obtained from the last counting position on the regular fuel plate, the standard plate would then be counted again. The activity measurements at the PRCF would then be terminated after the background data for both the decay and scan channels were recorded. All of these data were recorded as a function of the time of day.

A. CLEAN CRITICAL ASSEMBLIES

The initial critical loading in the PRCF consisted of 16-1/2 stationary fuel elements. These were positioned centrally within the reactor tank lattice structure in a 3 × 5-1/2 box array as shown in Figure 7. No shim assemblies were included in this clean, critical core. The approach-to-critical was performed by loading partially filled elements into the

CRITICAL ASSEMBLIES

CORE No. 1

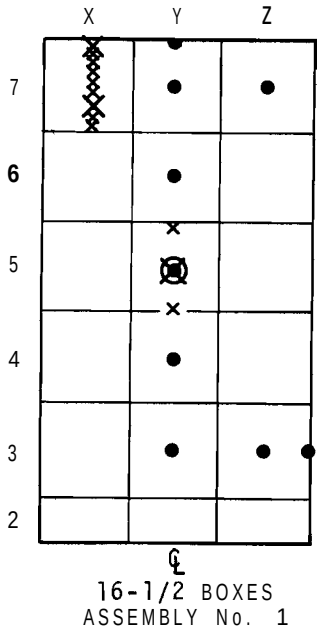

16-1/2 BOXES
ASSEMBLY No. 1

CORE HORIZONTAL MIDPLANE

× GAMMA SCAN - N-S DIRECTION - Z-7, Y-5
● COPPER PIN - CENTER AND EDGE AS INDICATED

VERTICAL PROFILES

× GAMMA SCAN - CENTER AND EDGE Y-5, X-7
○ COPPER PIN - CENTER ELEMENT Y-5
□ COPPER PIN - BERYLLIUM REFLECTOR AT 2" INTERVAL

CORE No. 2

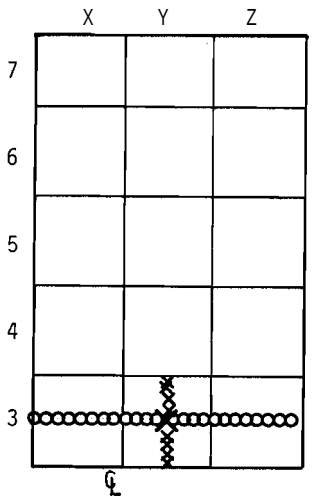

14-1/4 BOXES
ASSEMBLY No. 2

CORE HORIZONTAL MIDPLANE

○ GAMMA SCAN - E-W DIRECTION - X, Y, Z-3
× GAMMA SCAN - N-S DIRECTION - Y-3

VERTICAL PROFILES

× GAMMA SCAN - CENTER ELEMENT, Y-3

FIGURE 7. Location of Activity Measurements in PRCF–Phoenix Critical Assemblies Using Only Stationary Fuel Elements

reactor tank at each step. Three partial assemblies were loaded into the same column of the core lattice structure and each incremental step loading was equivalent to adding a total of eight plates or 1/2 of a stationary fuel box. Criticality with this core was achieved after loading X, Y, and Z-3, 4, 5, 6 and 7 with complete stationary fuel elements and X-2, Y-2, and Z-2 with assemblies that contained eight plates each. An irradiation was performed with this core loading to determine thermal flux distributions from copper pin activations and to determine power distributions by gamma scanning fission product activities in the fuel plates. The locations of these activity measurements are shown in Figure 7. The measured distributions and the flux and power results from a two-dimensional (2-D) calculation using the code EXTERMINATOR[13] are compared in Figures 8 and 9. The activity profile to be associated with an East-West midplane traverse is shown in Figure 8. This traverse crosses the center of the core through X-5, Y-5 and Z-5 and continues into the beryllium reflector. The profile that is obtained from a North-South midplane traverse is shown in Figure 9. This traverse crosses the center of the core through Y-2, 3, 4, 5, 6 and 7 and continues into the moderator at the edge of the fuel core.

The measurements for this clean core configuration were completed as scheduled. The shims and remaining fixed assemblies were then loaded to obtain the initial 3 × 9 full core. The experimental program and measurements which were obtained from this core are discussed in Sections II, IV and V of this report. This fuel was then unloaded, and the core structure was removed from the PRCF in order to permit restacking of the beryllium reflector in the region between the core tank wall and the safety sheet thimbles. Upon completion of this task, the restacked region presented a nearly solid beryllium

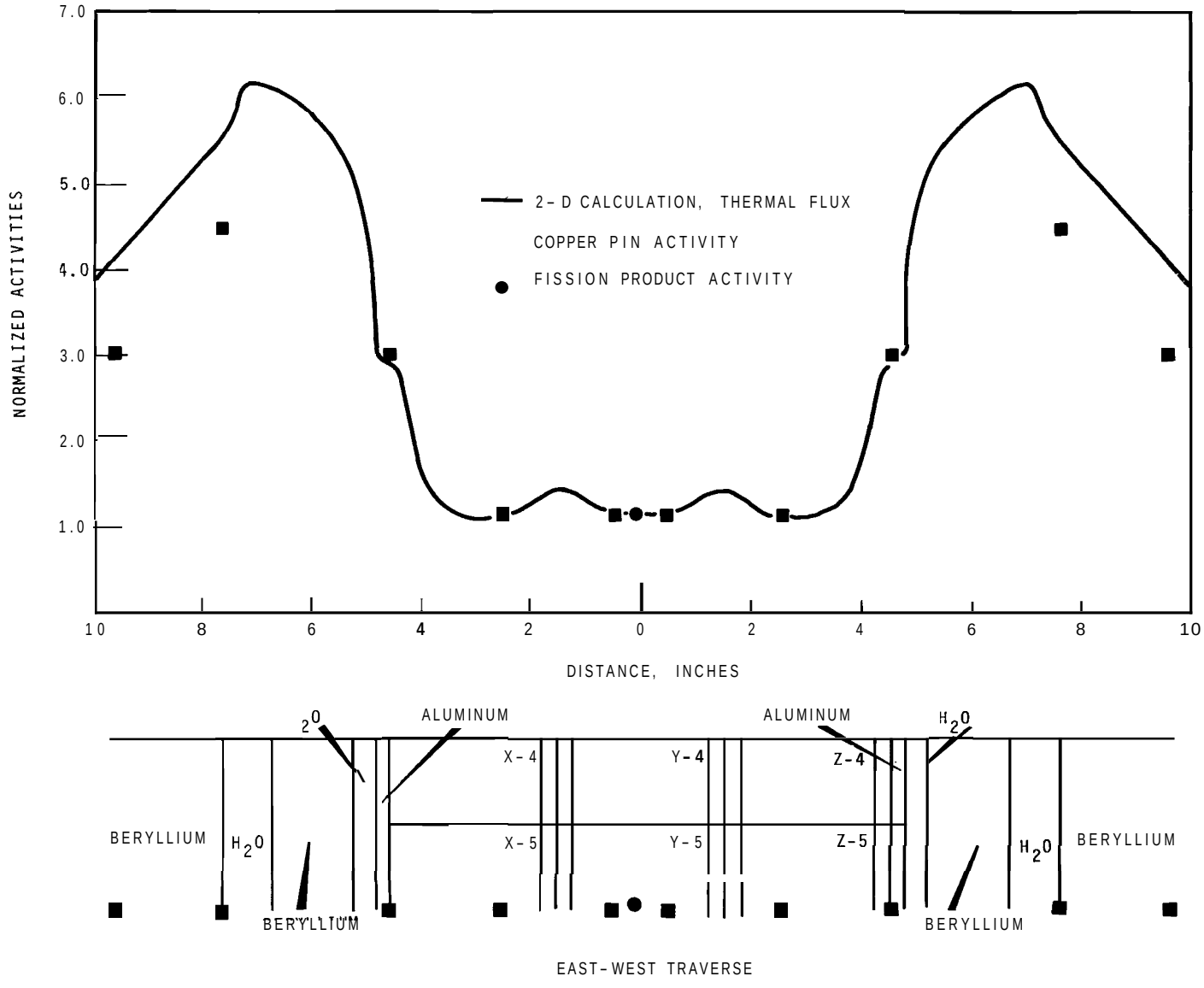

FIGURE 8. Midplane Traverse in East–West Direction of a Clean Core with 16–1/2 Stationary Fuel Elements

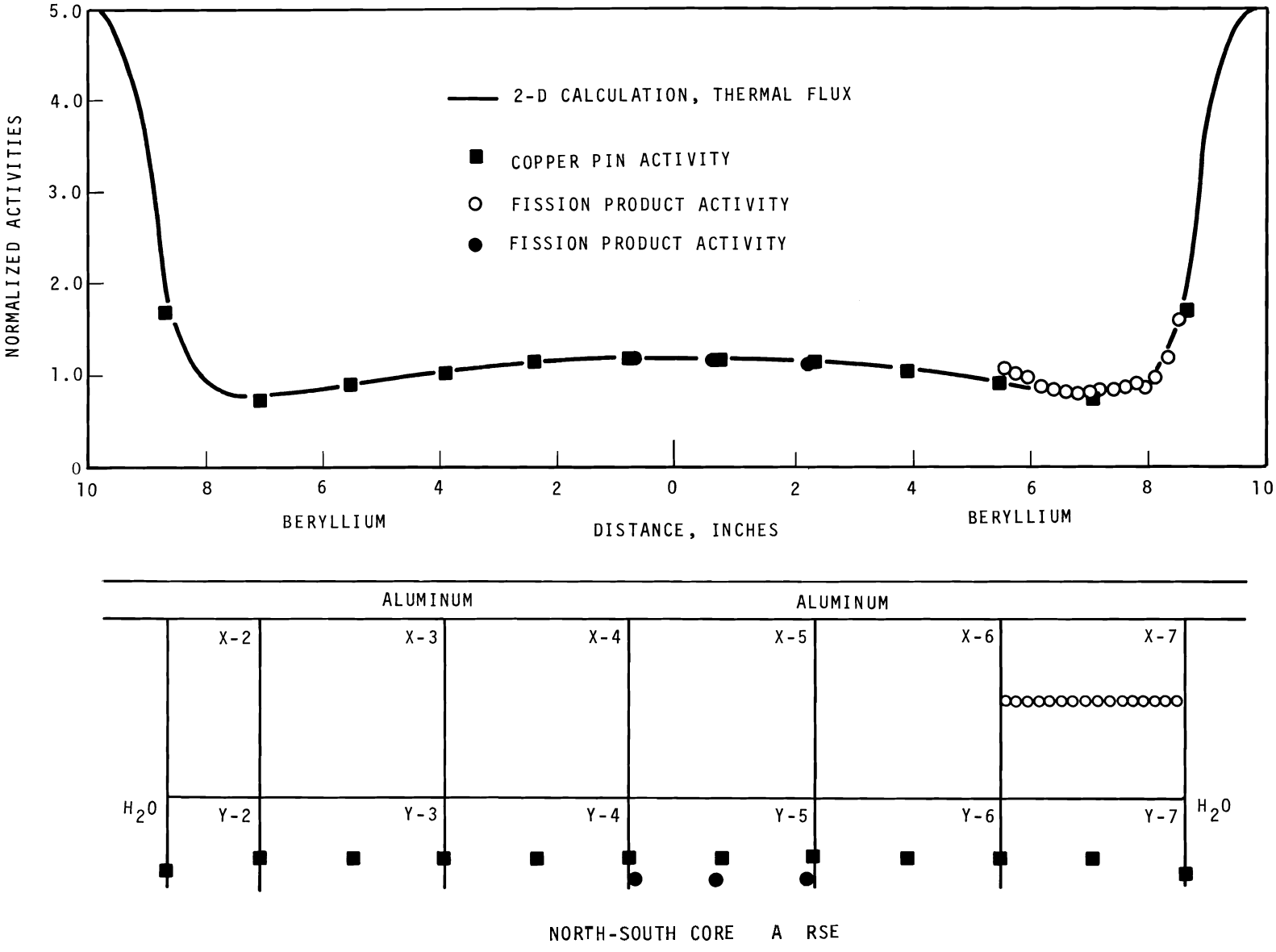

FIGURE 9 Midplane Traverse in North-South Direction of a Clean Core with 16-1/2 Stationary Fuel Elements

region at the core-reflector interface. As initially stacked, this region contained about 30% H_2O, and this change significantly improved the similarity between the beryllium reflector in the PRCF-Phoenix core and the reflector planned for the MTR-Phoenix core. After restacking the beryllium and boiling the fuel elements, a new shim-free critical loading was achieved with 14-1/4 stationary fuel boxes arranged in a 3 × 4-3/4 box array. These stationary fuel elements were positioned centrally within the reactor tank structure as shown in Figure 7. Complete fixed boxes were located in core lattice positions X, Y, Z-3, 4, 5 and 6 and partial assemblies that contained 12 plates each were positioned in X-7, Y-7 and Z-7. An irradiation was performed with this shim-free loading and the power distribution again was determined in the fuel plates by scanning the fission product activities in the plates. These measurements were obtained by utilizing the gamma scanning facility at the PRCF with the aperture width set for an ~1/4-inch resolution. The locations of these activity measurements are shown in Figure 7.

A three-dimensional power traverse of this shim-free core was completed, and these power shapes were then normalized to the previous shim-free core power distributions for comparison. The measured power distribution is illustrated in Figure 10 for an East to West lateral traverse across the centerline of the elements that were positioned in X-3, Y-3 and Z-3 at the core horizontal midplane. A midplane traverse from North to South across the centerline of the element that was located in position Y-3 is given in Figure 11. The measured power distribution is shown in Figure 12 for an axial traverse at the vertical centerline of the element in position Y-3 of this core.

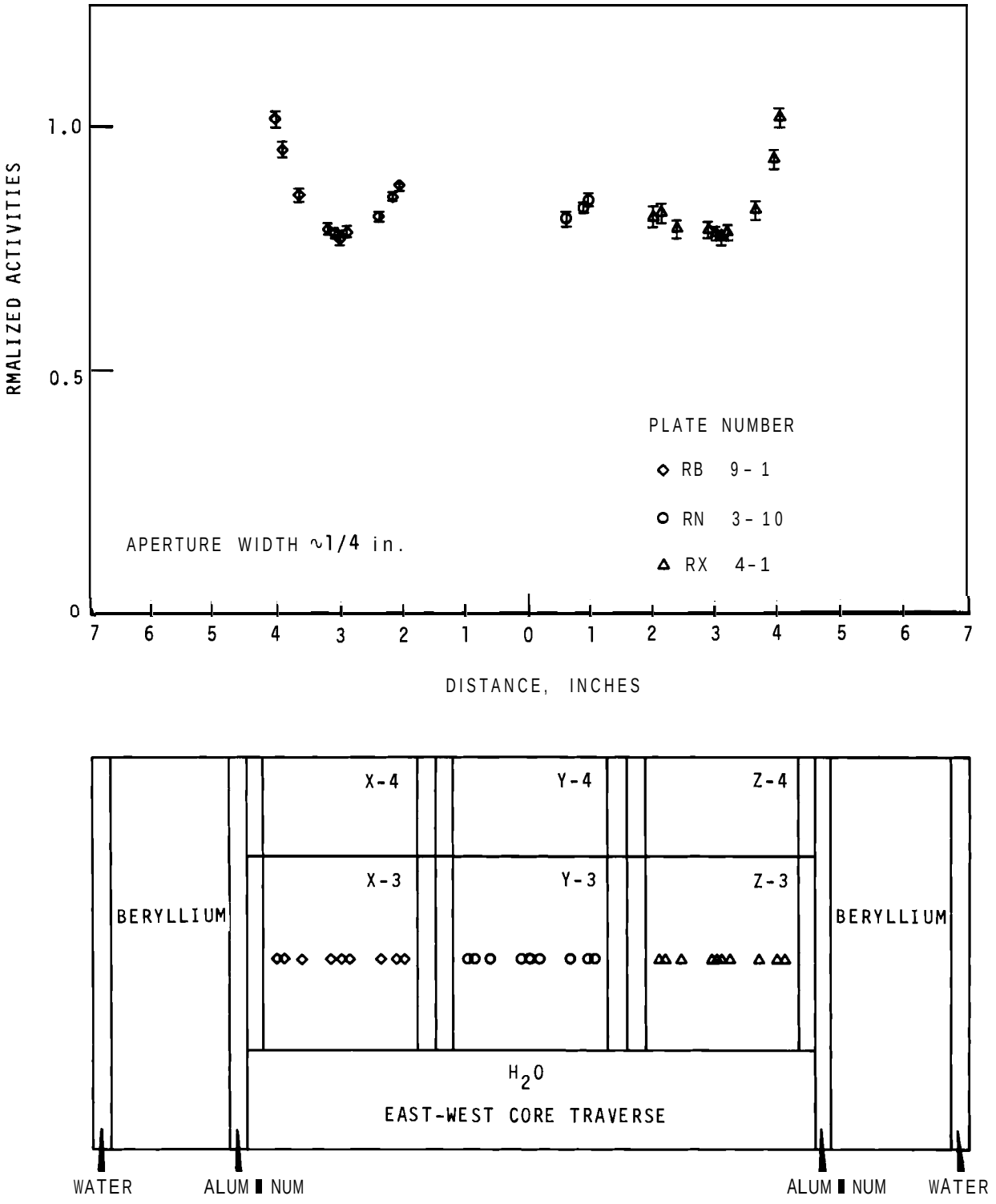

FIGURE 10. Lateral Traverse in East-West Direction of a Clean Core with 14-1/4 Stationary Fuel Elements

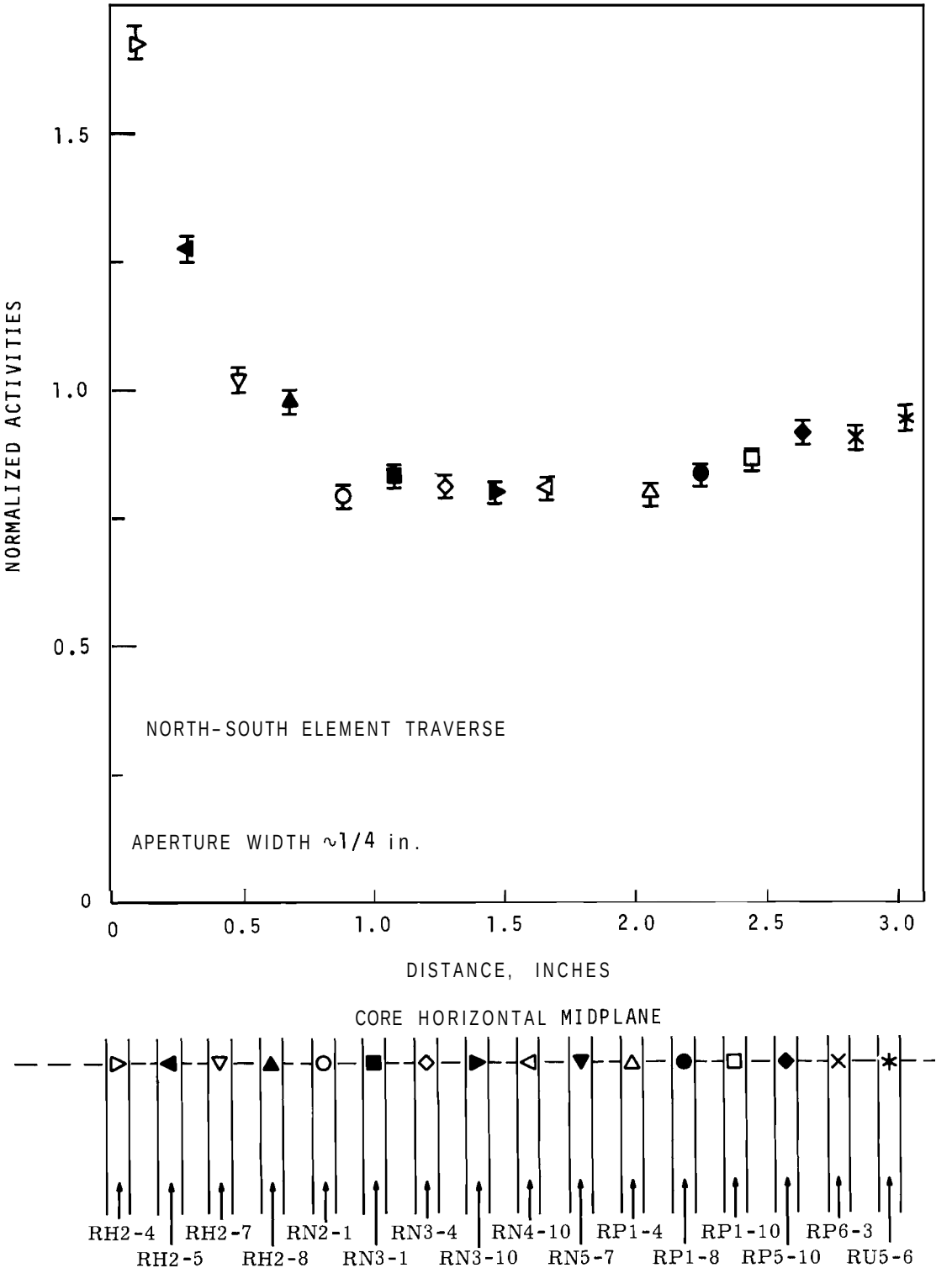

FIGURE 11. Midplane Traverse in North-South Direction at Position Y-3 of a Clean Core with 14-1/4 Stationary Fuel Elements

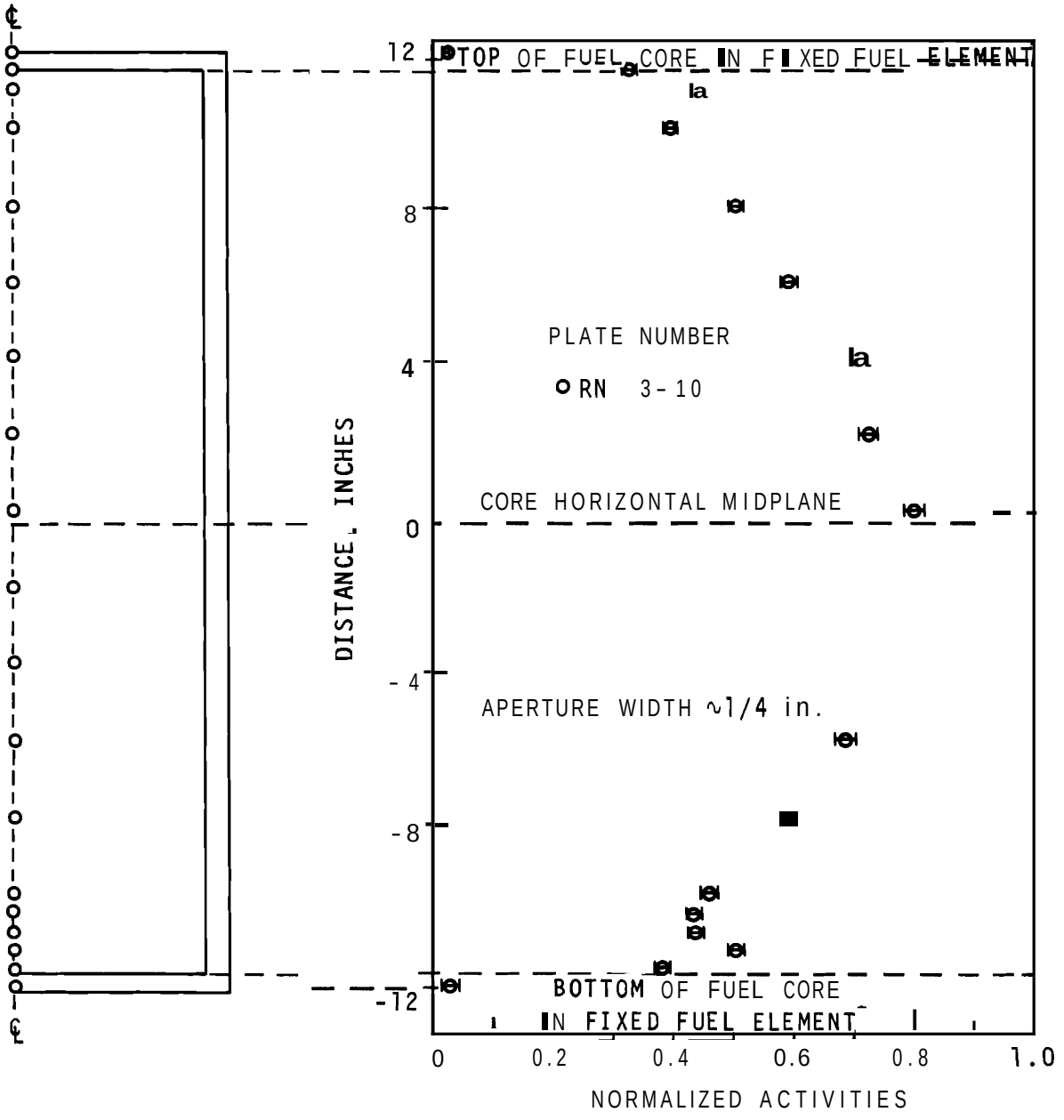

FIGURE 12. Axial Traverse at Midplane of Center Plate at Position Y-3 of a Clean Core with 14-1/4 Stationary Fuel Elements

B. SINGLE SHIM ROD CRITICAL ASSEMBLY

An additional critical core was constructed in the PRCF with the fuel which involved two major loading variations within the reactor lattice structure as compared to the previous clean critical core (Figure 7). The stationary fuel assemblies in this core loading were positioned adjacent to the beryllium reflector, and in addition to these elements, it consisted of only the cadmium section from one of the shim control rods. This special loading was designed to provide data from a core configuration that would be more amenable to calculation. The shim rod without the fuel follower was placed in position Y-1, and a symmetric array of 15-5/8 stationary fuel elements was loaded about it to obtain criticality as illustrated in Figure 13. This critical array was produced using complete as well as partial assemblies. The partial assemblies were loaded into core lattice positions X-6, Y-6 and Z-6 and contained 9, 8 and 9 plates, respectively. The complete stationary fuel boxes were located in X-1 and Z-1, as well as X, Y, and Z-2, 3, 4, and 5.

Irradiations were performed in this core configuration using gold and copper pin detectors to obtain bare and cadmium-covered activation profiles at the horizontal midplane. All of these detectors were made from the pure metal and were 0.25 inches long. The diameters of these pins were 0.020 inches and 0.035 inches for gold and copper, respectively. The pins were covered with 0.020-inch thick cadmium covers.

The cadmium ratios obtained from the results of these measurements are presented in Figure 13 as a function of reactor position for this core. All of the results are for saturation activities (that is, Cd ratio = $A_{\infty}^{Bare}/A_{\infty}^{covered}$) measured at the core midplane. The values for the gold and copper cadmium

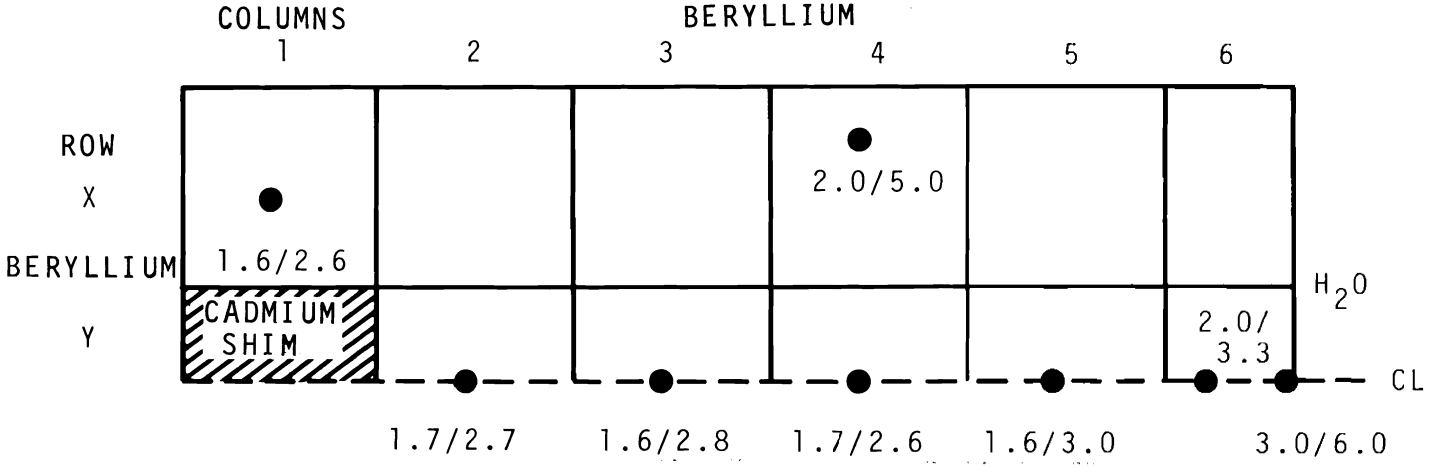

FIGURE 13. Spatial Values of Gold and Copper Cadmium Ratios from a Special Core Loading which Was Composed of Stationary Fuel Assemblies and the Cadmium Section of a Shim Rod

ratios are presented as gold/copper in Figure 13. The uncertainties in the gold cadmium ratios were observed to be ±1%, whereas the uncertainties assigned to the copper cadmium ratios were on the order of ±3%. These results indicate that the influence of the beryllium reflector is limited to the outer one-quarter of a fuel box, and that the spectral change due to the water region is limited to the outer one-half of a fuel box. These measurements have provided experimental data from a core with relatively simple geometry. This data will be used in testing the computational models and methods being developed for Phoenix fuel cores.

C. FUEL CORE CRITICAL ASSEMBLIES

The initial full-core critical loading consisted of 19 stationary fuel assemblies and 8 shim control rods which were located in the reactor lattice positions as shown in Figure 1. The approach-to-critical was performed by incrementally withdrawing the shim rods as a bank, and the critical height was achieved with the shims withdrawn to 65%. Gamma scan data were obtained at various positions within this core, and these are illustrated in Figure 14. The decision to restack the beryllium reflector had already been made; therefore, extensive measurements were not performed within this particular core. The measurements that were made in this core were designed to yield only qualitative information on the characteristics of this type of fuel loading. This core loading contributed substantial information on the expected shapes of the power distributions within the shim rod fuel followers and stationary fuel boxes. In addition, operational procedures were identified and changed in order to ensure continuity of the planned Phoenix Experimental Program.

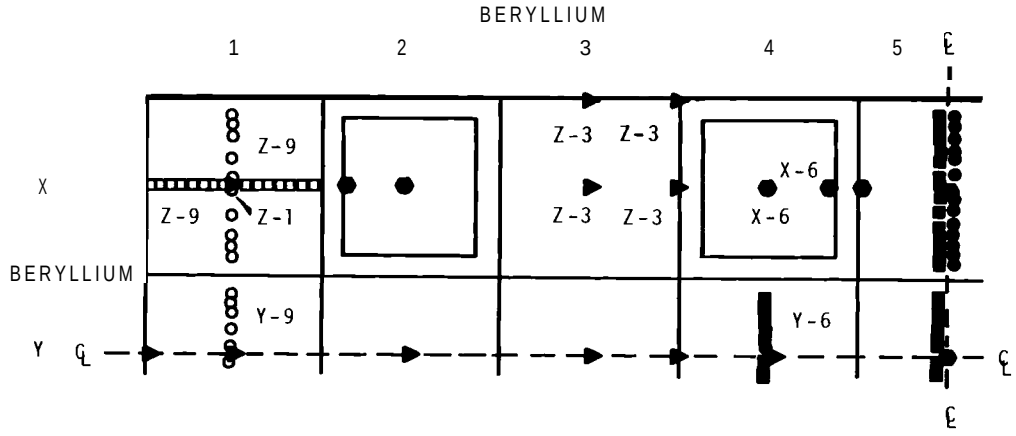

CORE HORIZONTAL MIDPLANE

○ GAMMA SCAN - 27 BOX CORE No. 1 - E-W DIRECTION - Y-9, Z-9

□ GAMMA SCAN - 27 BOX CORE No. 1 - N-S DIRECTION - Z-9

GAMMA SCAN - 27 BOX CORE No. 2 - E-W DIRECTION - X-5, Y-5, Y-6

6 INCHES BELOW CORE HORIZONTAL MIDPLANE

● GAMMA SCAN - 27 BOX CORE No. 2 - E-W DIRECTION - X-5

> COPPER PIN - 27 BOX CORE No. 2 - CENTER AND EDGE OF ELEMENTS AS INDICATED

VERTICAL PROFILES

● GAMMA SCAN - 27 BOX CORE No. 2 - CENTER AND EDGE OF ELEMENTS X-5, Y-5, X-6, X-2

COPPER PIN - 27 BOX CORE No. 2 - BERYLLIUM REFLECTOR AT 2 in. INTERVALS FROM CORE

FIGURE 14. Location of Activity Measurements in the Full 3 × 9 Shimmed Cores. (The Core Locations Z-1, Z-9, etc. designate the measured positions in this core.)

After restacking the reflector at the core reflector interface, a new full core critical loading was achieved with the shims in this 3 × 9 array withdrawn to 59%. An extensive series of irradiations were performed with this core configuration to provide both y-scan and copper pin activity measurements. Quantitative information has been obtained from these measurements on the relative shapes and magnitude of the power profile in the shim rod fuel followers and fixed boxes, as well as the reflector. The reactor positions at which activation data were obtained in this second full PRCF-Phoenix core configuration are illustrated in Figure 14. These measurements have been used to extrapolate to the flux and power distributions that were expected in the normally shimmed Phoenix fuel core at initial startup in the MTR.

1. Power Profiles for Stationary Elements

The relative power distributions inferred from the centerline scans obtained from two of the plates located in the element that was positioned in X-5 are shown in Figure 15. The data presented here for the interior plate (RG 2-3) and the exterior plate (RP 2-10) have been normalized by taking the ratio of a point of the measured activity to the core average (that is, $A_i/\bar{A}_{core}$). It was noted that the axial power traverses of these plates have shapes that are similar in profile to the regular MTR-banked shim traverses at startup. These traverses have shown that the axial peak power on the outside plate is located about 5 inches above the bottom of the fuel core whereas the power spike appears at the bottom edge of the interior plate. The depressions in the power profiles obtained for the region adjacent to the cadmium section of the banked shims show very prominently in Figure 15. The relative values in this region are a factor of ten in magnitude below the peak values.

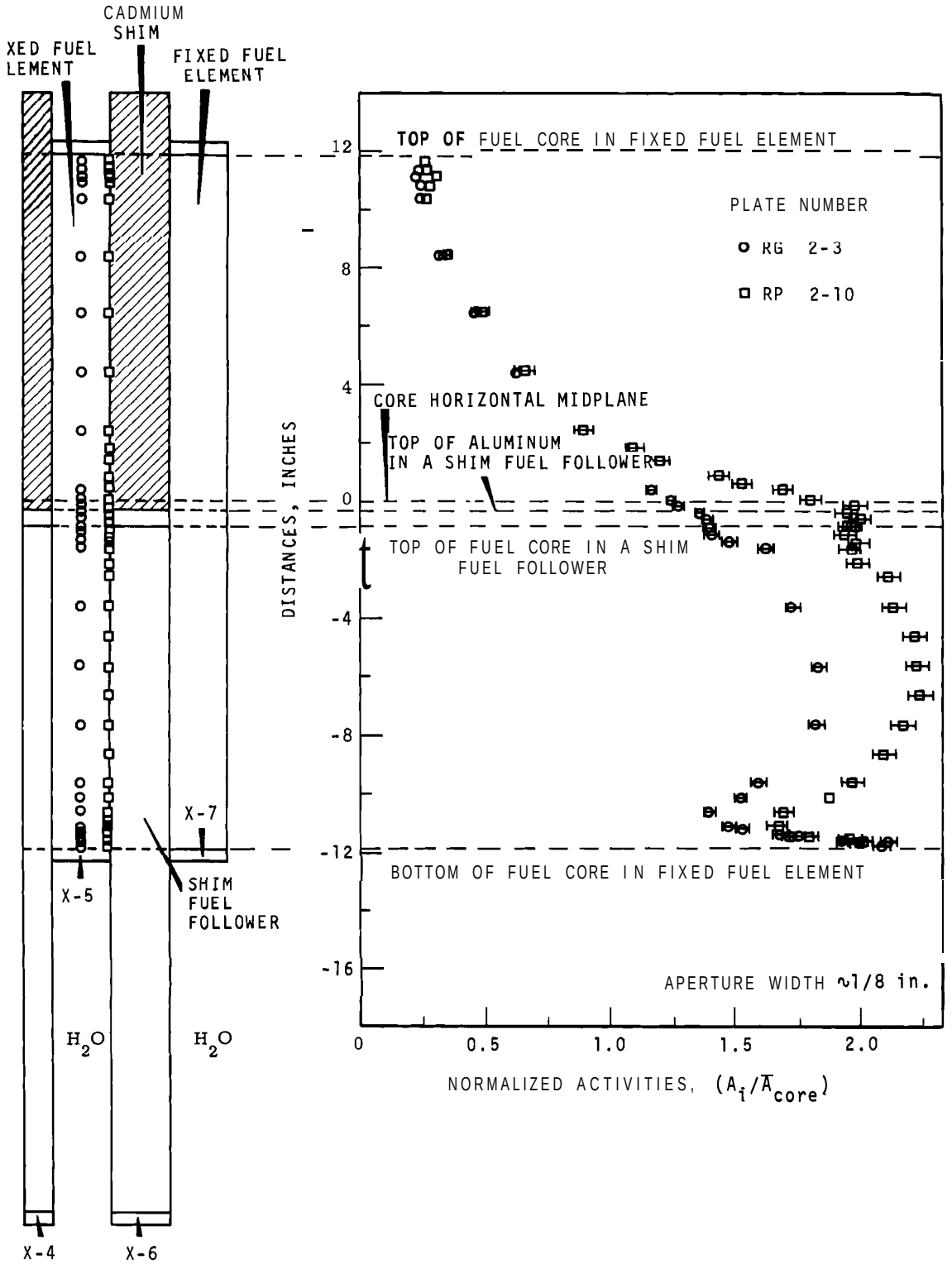

FIGURE 15. Axial Power Profiles from Plates of a Stationary Fuel Element Located at X-5 in the Full Core Loading with Banked Shims at 59% Withdrawn

2. Power Profiles for Shim Fuel Follower

The axial power distributions through the centerline of an exterior plate (RR 3-2) and an interior plate (RR 3-7) were obtained from the shim rod fuel follower which was located at X-6. These are illustrated in Figure 16. This data shows that the power profiles in both plates increase to a peak again at about 5 inches above the bottom of the stationary fuel in the region adjacent to the fixed fuel. The traverse from plate RP 3-2 of the shim fuel follower also shows that the axial peak power on an outside plate is located 1 inch below the bottom of the fuel core in the fixed fuel element. Calculations were used to predict this power peak in the shim fuel followers below the stationary fuel core.

Scan measurements were made at the position of peak power on the shim fuel follower plates. These plates were sequentially removed and scanned to determine the plate-to-plate variations in the power peaks. A comparison of the scans obtained from the outside three or four plates of this shim showed that the magnitude as well as the shape of this peak was reduced. On the other hand, the traverse obtained from plate RR 3-7 shows that the peak no longer exists in the interior of the element. In addition, it should be noted that a continued power production is present in those plate sections positioned below the fixed elements in the core.

3. Composite Power Profiles for Fixed and Shim Elements

The composite profile of the adjacent exterior plates taken from a shim follower and stationary fuel element are illustrated in Figure 17. The profile of the fixed plate RP 2-10 (Figure 15) was combined with that obtained for the' shim plate RR 3-2 (Figure 16) in order to show the effects that the different regions of this core have on the resultant

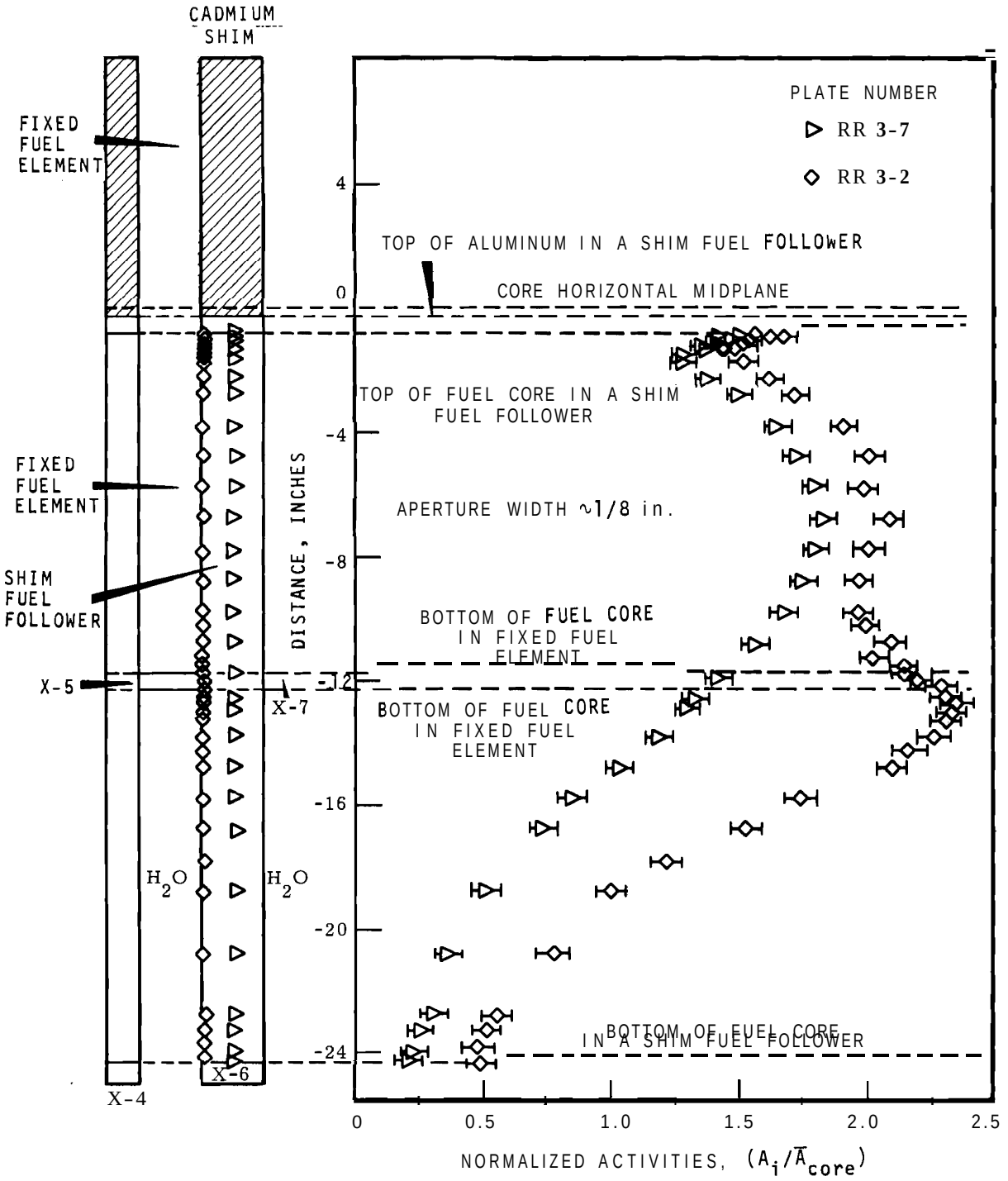

FIGURE 16. Axial Power Profiles from Plates of a Shim Fuel Follower Located at X-6 in the Full Core Loading with Banked Shims at 59% Withdrawn

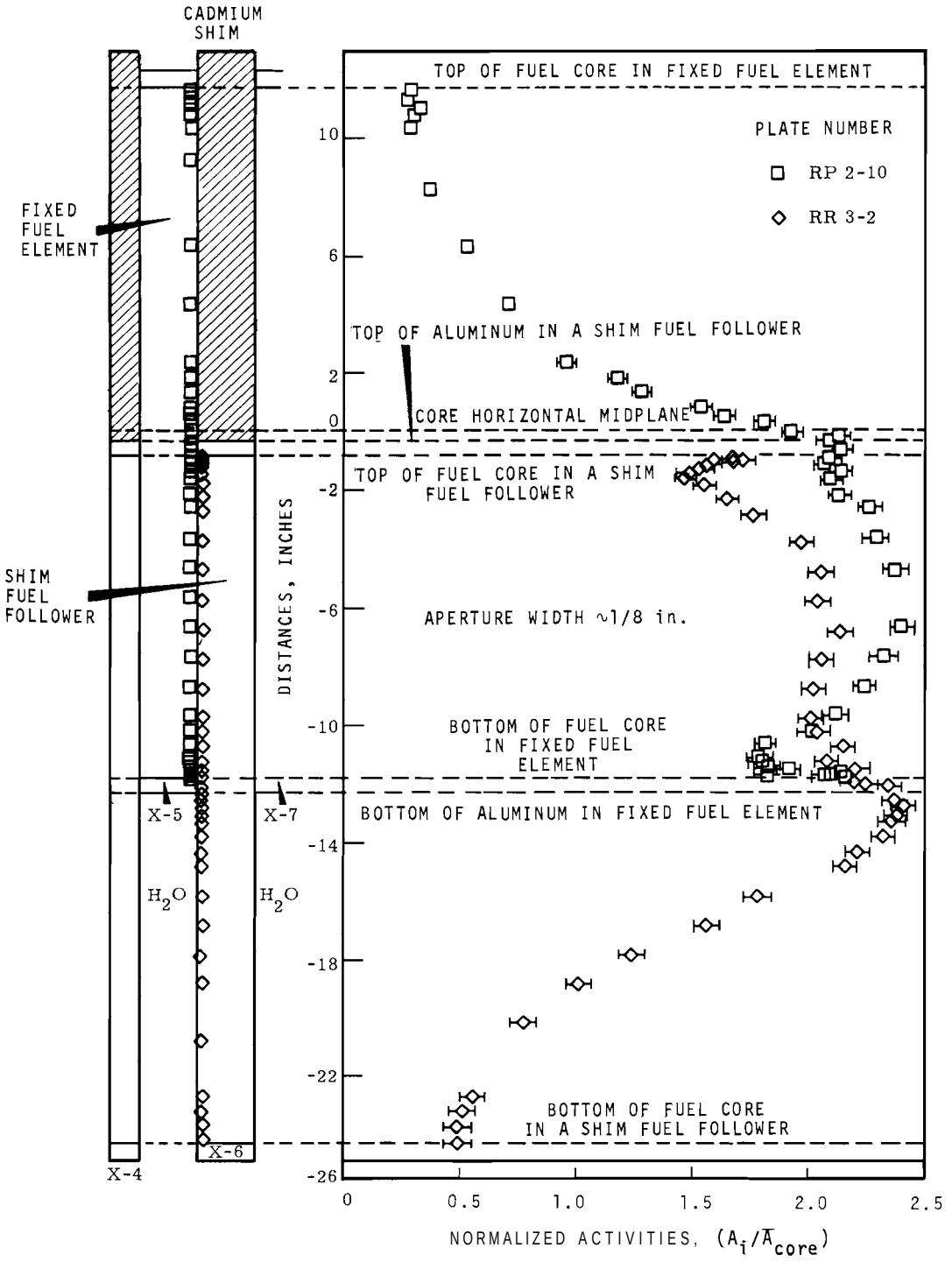

FIGURE 17. Axial Power Profiles from the Exterior Plates of a Shim Fuel Follower and Adjacent Stationary Fuel Element in the Full Core Loading with Banked Shims at 59% Withdrawn

power distributions. The magnitude of the peak observed from the shim fuel follower was found to be no greater than the peak observed in an exterior plate of the fixed element at the bottom of the core.

4. Comparisons of Calculations and Measurements

The activity measurements have assisted in determining the reliability of the calculational models used in the areas of localized flux and power peaking. For example, the measured axial power profile from an interior plate is compared in Figure 18 with the calculated[4] profile using the code WHIRLAWAY.[14] These curves have been normalized to equal areas. The calculation significantly overestimates the power peaking at the bottom edge of the core. Without the measurements, the calculations would have led to severe limitations on reactor power during the MTR burnup program.

5. Tapering Fuel Plates

Irradiations were also made with plates containing tapered fuel cores, and these results are compared with the data obtained from a standard fuel core in Figure 19. Six plates containing tapered fuel cores were loaded into the center of one of the stationary fuel elements in the reactor at lattice position Y-5. The fuel cores had tapers of 1-1/2 inches and 1/2 inch, respectively, at opposite ends of the plates. The standard fuel core was 0.04 × 2.50 × 23.5 inches, and the tapered plates were fabricated by linearly reducing the standard plutonium core from 0.040 to 0 inch over these effective lengths.

Two separate irradiations were performed to identify the changes in the power profiles that could be attributed to these tapered plates. These measurements definitely determined the effectiveness of the tapered fuel in further reducing the power

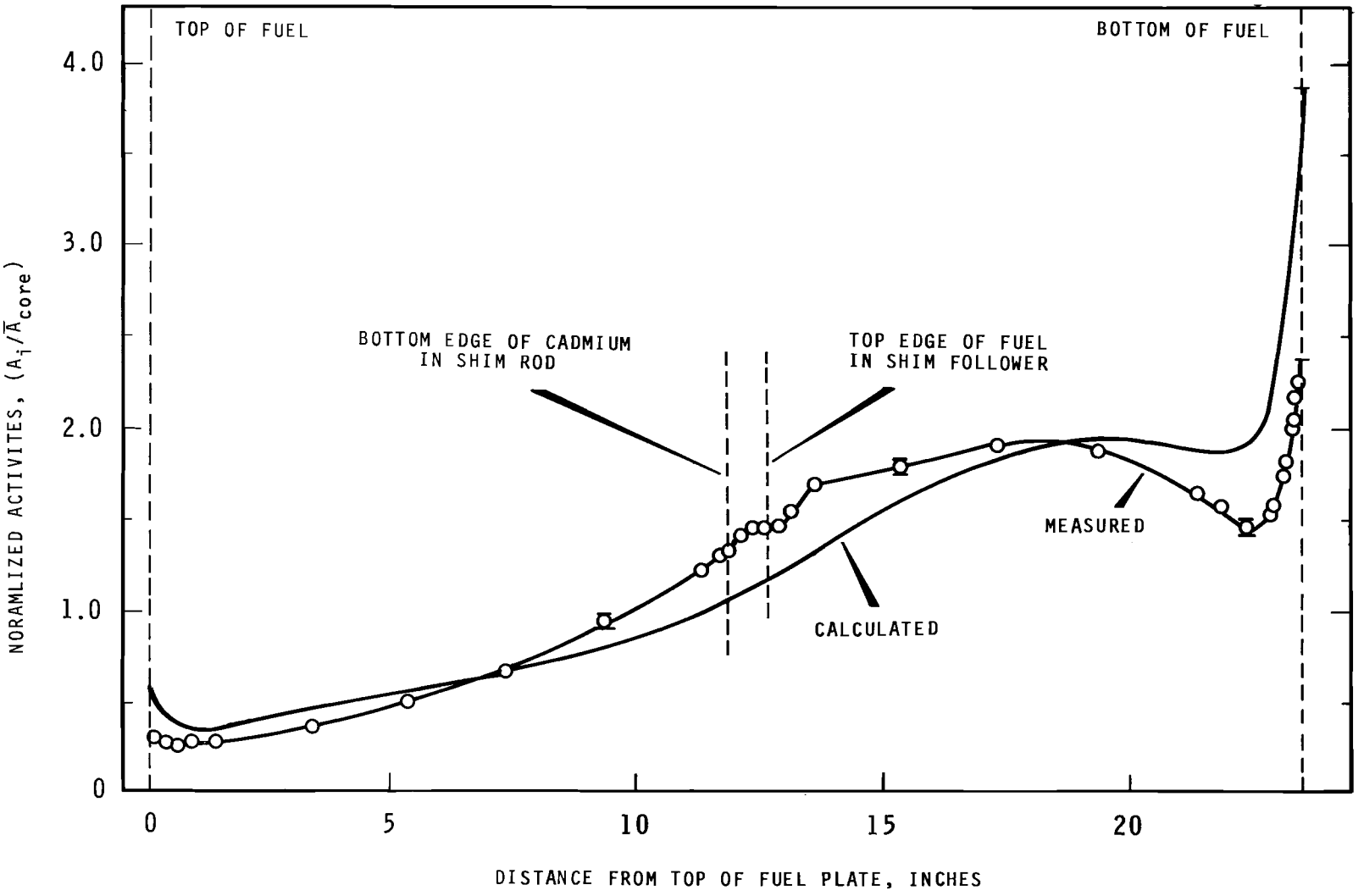

FIGURE 18. Comparison of Measured and Calculated Axial Power Profiles in the PRCF-Phoenix Core

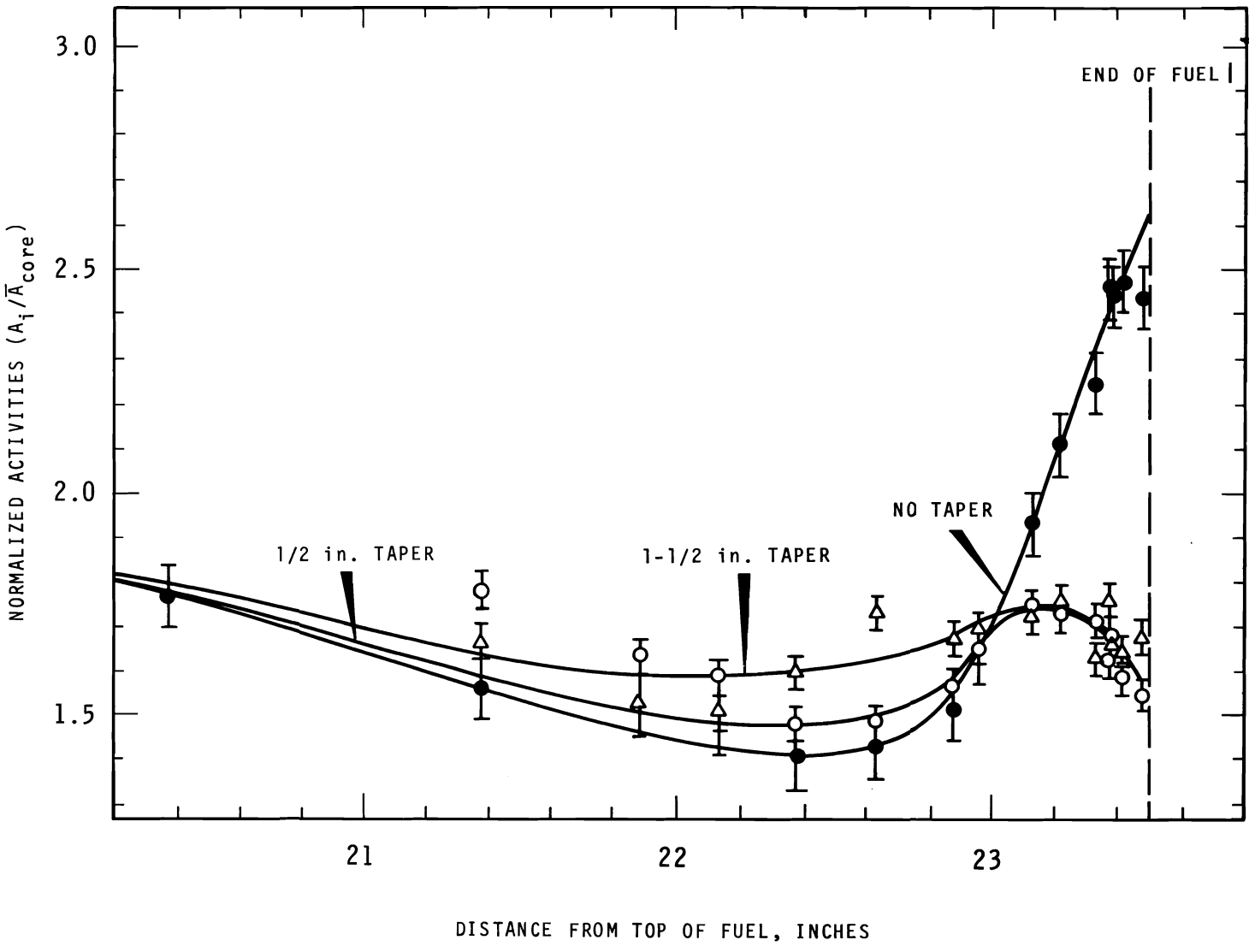

FIGURE 19. Reduction of Power Peaking by Tapering Fuel Cores in an Interior Plate of a Stationary Fuel Element Located at Y-5 in the Full Core with Banked Shims at 50% Withdrawn

spikes at the bottom of the core in a standard fuel plate. There is at least a 30% reduction in the power peaking at the bottom edge of the core due to the tapered plates. As a direct result of this experiment, all of the MTR-Phoenix standard fuel plates were tapered.

6. Power Profiles - Fuel Core Edge

As a part of this experimental program, the power peaking at the edge of the fuel core adjacent to the beryllium reflector was also investigated. For example, the relative power distributions inferred from the horizontal traverse of the central plate taken from two stationary fuel elements in lattice positions X-5 and Y-5 are illustrated in Figure 20. These data show the characteristic power peaking at the edge toward the beryllium reflector as previously observed in the clean critical assemblies.

7. Flux Traverse Data

Copper pin irradiations were also performed to obtain horizontal flux profiles across the core and reflector 6 inches below the core midplane. The locations of these copper pins within the reactor core are identified in Figure 14. A North-South activity profile was obtained through the center of the Y row and this is shown in Figure 21. An East-West traverse at the interface between the 3rd and 4th fuel columns was also measured. These data as well as the measurements that were made in the reflector in this plane are shown in Figure 22. Additional copper pin activities were measured to obtain vertical flux profiles at selected locations in the beryllium reflector. The relative axial flux distributions for some of these locations are illustrated in Figure 23. A comparison was made between the experimental data and a one-dimensional (1-D) HFN calculation[15] for the PRCF-Phoenix core, and these

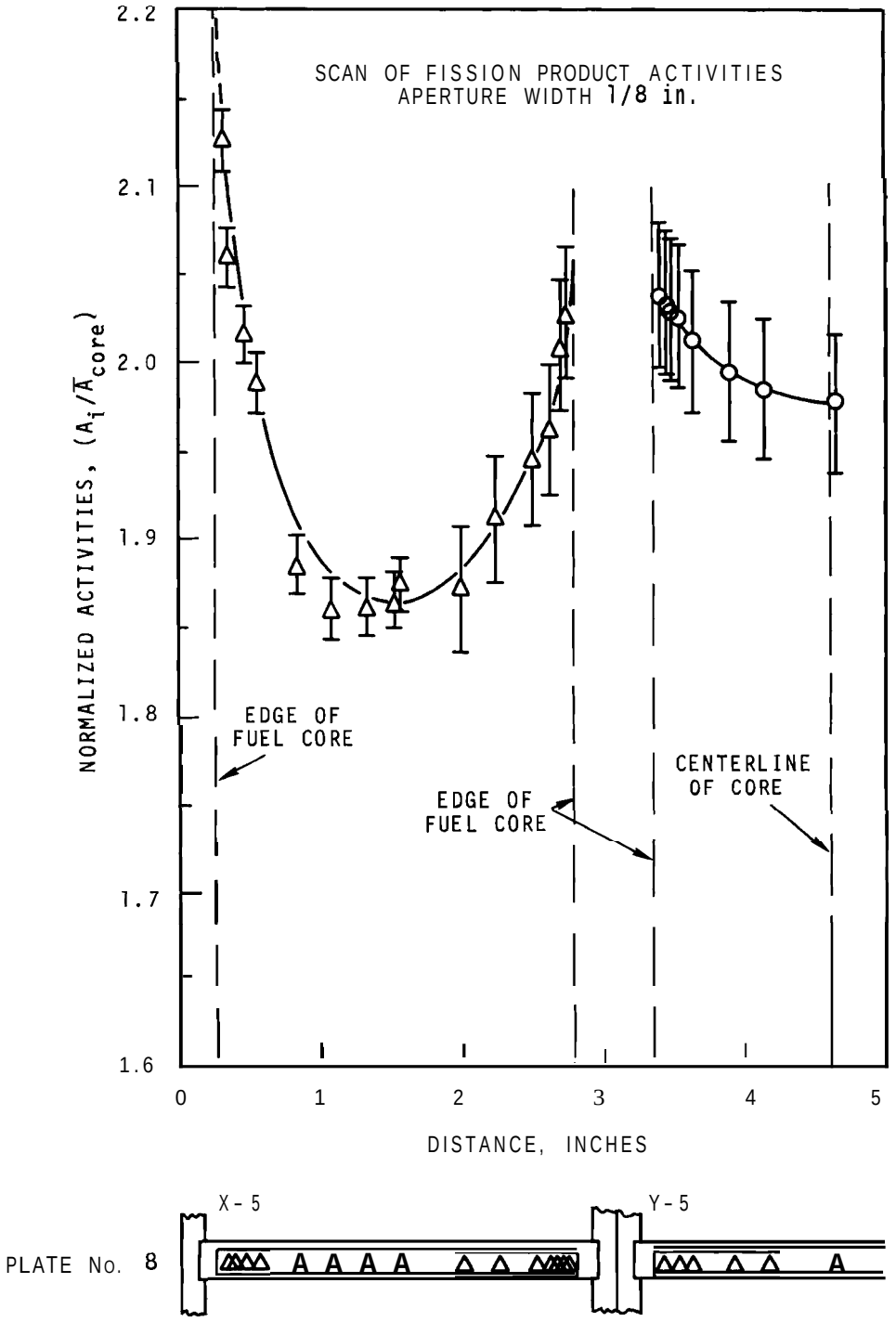

FIGURE 20. Lateral Traverse in East–West Direction at the Peak Power in the Full Core Loading with Banked Shims at 59% Withdrawn

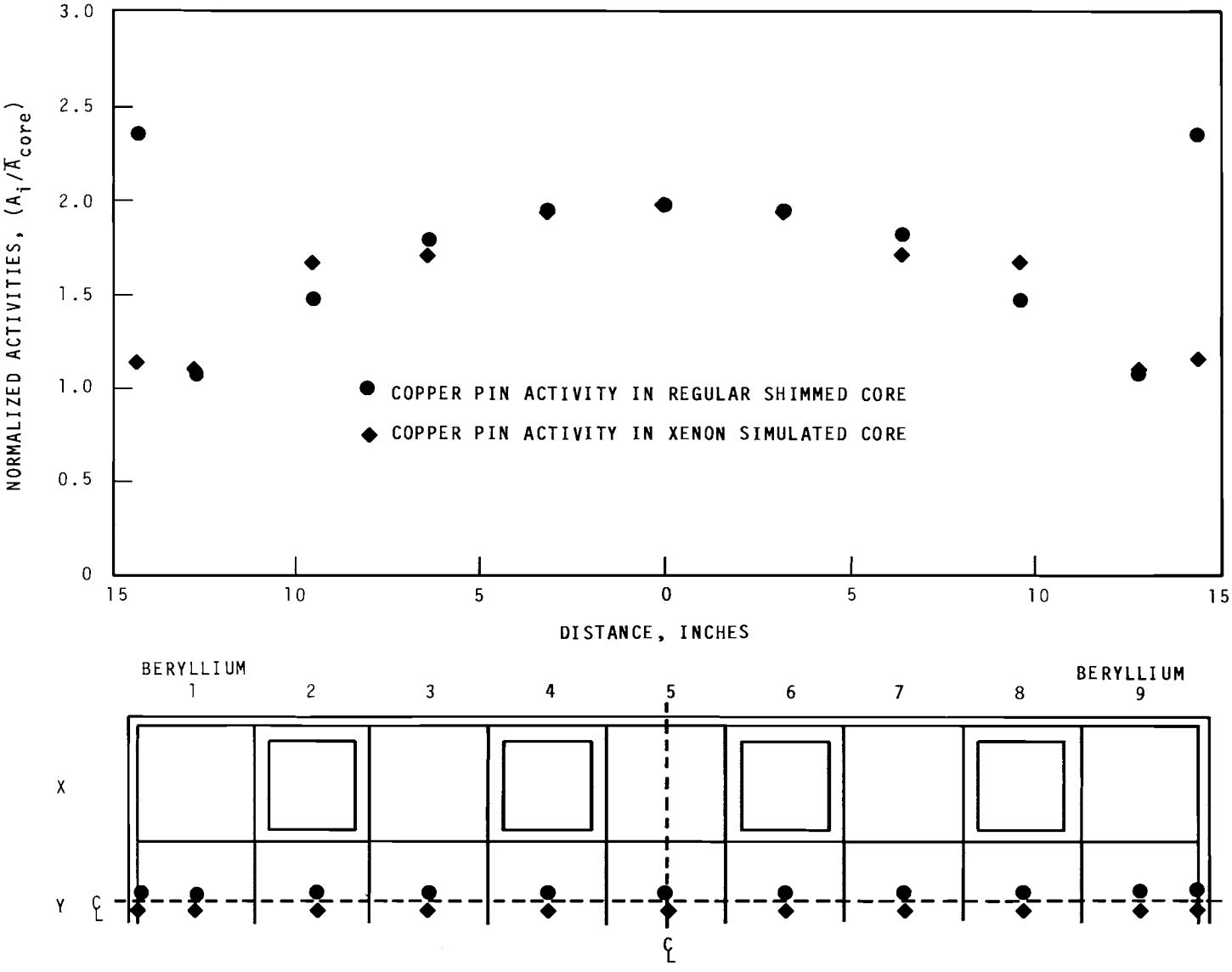

FIGURE 21. Lateral Traverse in North-South Direction at 6 Inches Below Core Horizontal Midplane

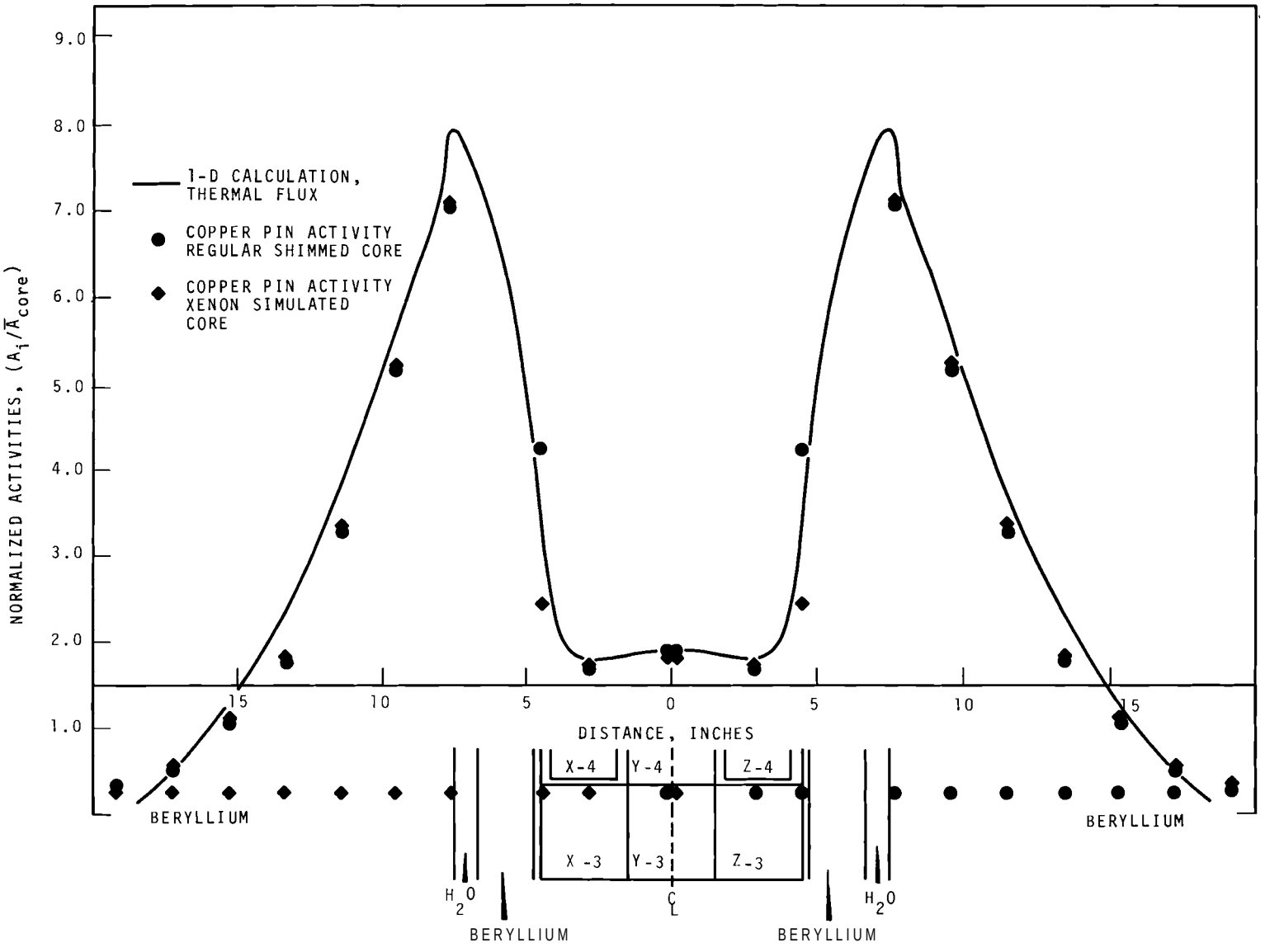

FIGURE 22. Lateral Traverse in East–West Direction at 6 Inches Below Core Horizontal Midplane

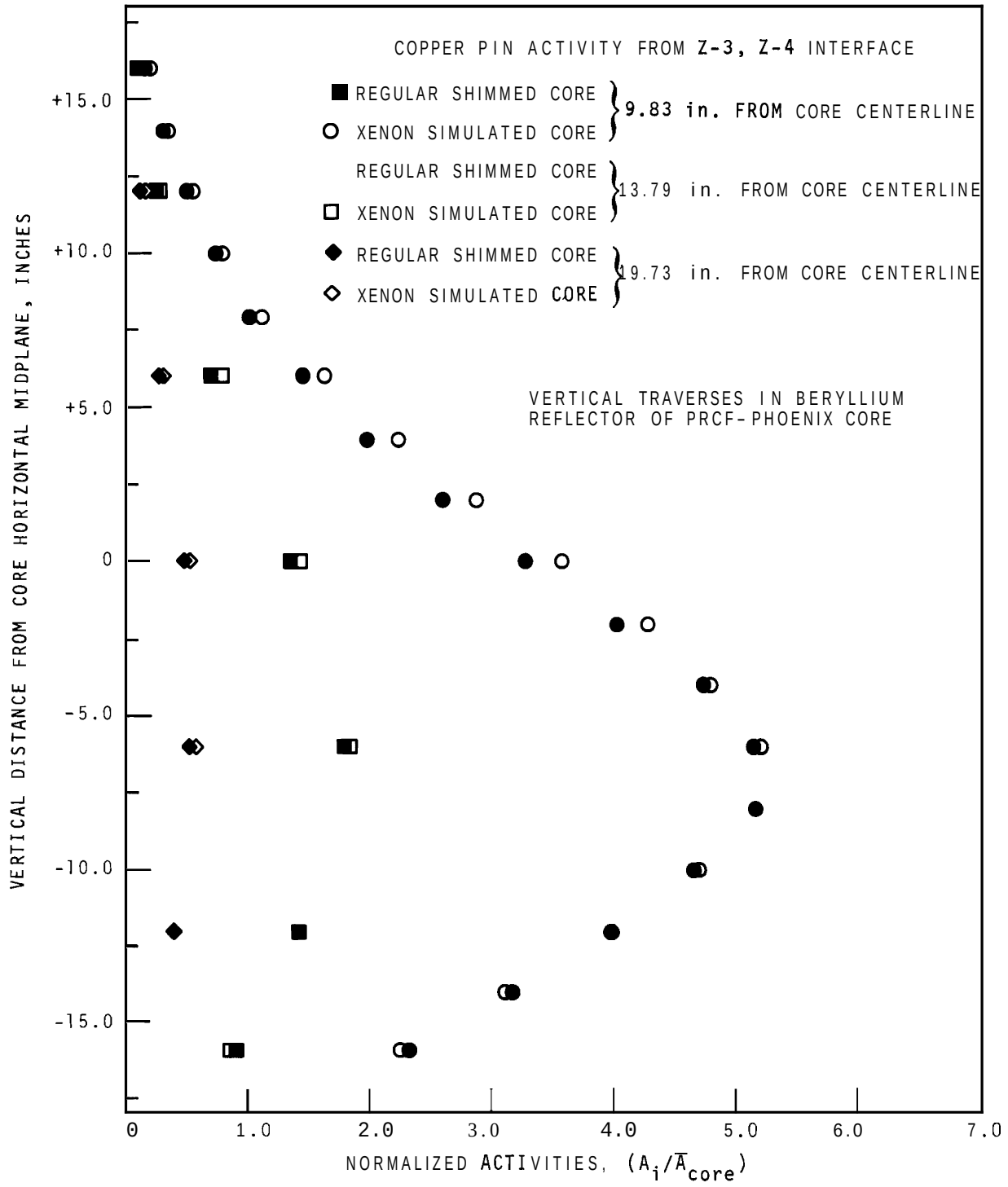

FIGURE 23. Vertical Activity Profiles in the Beryllium Reflector of the MTR–Phoenix Mockup of the PRCF

are shown in Figure 22. The calculated values were normalized to the measured flux distributions at a point 6 inches below the core midplane at the interface between the elements positioned at Y-3 and Y-4.

D. SIMULATED XENON-POISONED CORE

Borated polyethylene strips (0.005 × 2.5 × 23.5 inches). were inserted into the coolant channels of the stationary fuel elements to simulate partial xenon poisoning. The location of these strips within the coolant channels are listed in Table III. The total number of strips that went into each element are listed for each lattice position in Figure 24. Distribution of 88 strips of this material throughout the core produced a banked shim critical height of 62.8% withdrawn, or an effective poisoning worth of 15 mk.

TABLE III. Location of the Borated Strips Within the Coolant Channels of the Stationary Fuel Elements

Number of Borated Strips	Number of Fuel Elements That Have This Number of Strips	Coolant Channel Number
3	4	4, 8, and 12
4	3	2, 6, 10, and 14
5	8	2, 5, 8, 11, and 14
6	4	1, 3, 6, 10, 13, and 15

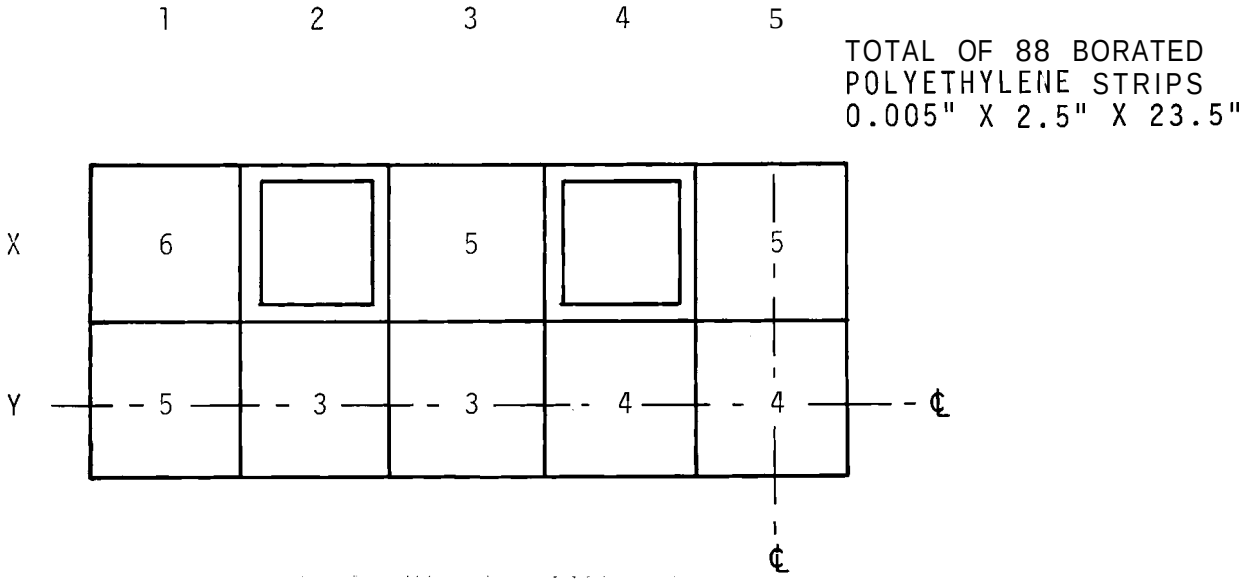

FIGURE 24. Total Number of Borated Strips Within Each Lattice Position of the Phoenix Fuel Core

The results of measurements of flux and power profiles obtained in the poisoned core have been normalized for comparison with the normal shimmed core measurements and with calculations. The results of the gamma scanning measurements indicate that the maximum axial flux is located 6 inches below the core horizontal midplane in position Y-5. This is consistent with the data obtained from the unpoisoned core measurements. Additional irradiations were made in this poisoned core configuration to obtain horizontal pin activity profiles throughout the core and the beryllium reflector at 6 inches below the horizontal midplane. Copper pins were also activated to obtain the vertical flux profiles in the beryllium reflector at selected distances from the core in the poisoned loading for comparison with results from the unpoisoned loading. The results of the copper pin activities imply that the buildup of xenon poisoning in the core will tend to reduce the flux peak in the fuel adjacent to

the beryllium reflector and cause an overall flattening of the power distribution in the core, as shown in Figures 21 and 22. The flux profile from a 1-D calculation using the code HFN[15] has been normalized to the measurements obtained from the poisoned and unpoisoned core configurations 6 inches below the core midplane at the interface between the elements in Y-3 and Y-4. The comparison of the measured and calculated results is given in Figure 22. The results of the normalized flux profiles show that the thermal flux reaches a peak in the beryllium reflector about 3 inches from the reactor tank wall. The axial flux profiles in the beryllium reflector from both the poisoned and unpoisoned cores are shown in Figure 23. The flux profiles in this region also indicate that a maximum occurs 6 inches below the horizontal midplane of the core, which is consistent with the shape of the power distributions in the fueled region of the core.

VI. PRCF-PHOENIX CORE POWER MAP

The flux and power distributions generated as part of the MTR-Phoenix fuel mockup critical experiments have also been analyzed to obtain: power fractions in each fuel element, the peak-to-average power fractions, and three-dimensional power distributions. The magnitudes and locations of the hot spots in the core were determined. The values of the maximum power points, A_i/A_{core}, were found to be about 2.4 to 2.5. These data have been. used as input to an analysis of heat transfer in the core and the thermal hydraulic design analysis to determine the allowable operating power level for the Phoenix fuel core in the MTR.

A comprehensive analysis of the results of all the gamma scan and copper pin activity data for the MTR-Phoenix fuel mockup experiment in the shimmed core was made to develop a detailed three-dimensional (3-D) power map with the average power in the core normalized to be equal to 1.0. This analysis required the correlation of the experimental data from throughout the core, the determination of the unique power shapes for all core positions, and the verification of the assumption of core symmetry. All of the measured data were used in constructing the 3-D power shape in the core, which was integrated to obtain the total core power. Some extrapolations were necessary to construct the 3-D profile, since data were not obtained from all points of interest in the core. All extrapolations and assumptions were made on the conservative side; maximum values of peaking were assumed if not measured directly. The value of the power peak located along the vertical centerline of each element was used as the point of normalization. The profiles along the vertical axis, the N-S axis, and the E-W axis pass through this point. A volumetric average power was then

generated for each fuel element and shim fuel follower in the core, and then for the whole core. Each data point was then normalized by dividing by the core-average value. The percent of power per element is presented in Figure 25 as a function of the position of the elements in the reactor core. The element producing the most power is seen to be located in X-5 or as reflected into Z-5 by symmetry. The estimated uncertainties in these power values are ±10%.

The peaking factors that are to be expected of this core for a center fuel plate and an outside fuel plate in the position X-5 are listed in Table IV.

The hot spot in the shim fuel follower was located on the outside fuel plate 1 inch below the stationary fuel in the core. The ratio of the peak power to core average for this position was observed to be 2.4. The ratio of the peak power to core average at the bottom of the fixed fuel plates was reduced as shown in Figure 19 from 2.5 to 1.5 by tapering the fuel cores in the plates. This eliminated the location as a hot spot in the core.

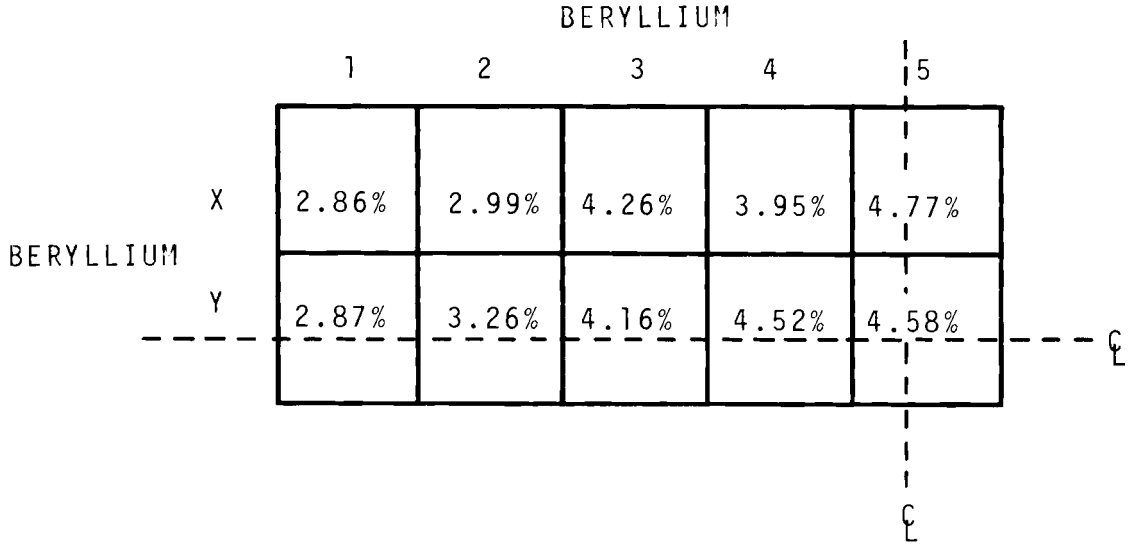

FIGURE 25. PRCF–Phoenix Core Percent Power Per Element

TABLE IV. PRCF–Phoenix Core Peaking Factors for Center and Outside Fuel Plate from Position X–5

Plate From X-5	Location of Peak Power	$P_i/\overline{P}_{core}$	Source of Data
Center	C_L of Plate	1.87 ± 0.04	Measured
Center	Be-edge of Plate	2.2	Extrapolated from measured data
Outside	C_L of Plate	2.28 ± 0.05	Measured
Outside	Be-edge of Plate	2.3	Minimum lower bound, assuming no variation in the shape from the center of this plate to its edge.
Outside	Be-edge of Plate	2.7	Maximum upper bound, assuming no changes in the shape observed of the central plate from its center to the Be-edge.
Outside	Be-edge of Plate	2.5	Average between minimum and maximum bound.

Results of this analysis have provided input for the preliminary thermal hydraulic and heat transfer analysis of the Phoenix fuel core in the MTR.[5] Comprehensive axial profiles were generated to describe five lateral positions across each plate for the three stationary fuel elements in X-5, Y-5, and Y-6 and for the shim fuel follower located at X-6. These are equivalent to MTR positions L-25, L-35, L-36 and L-26, respectively. The power profiles formed the basis of the heat transfer analysis. The MTR startup power distributions based on the PRCF experiment show maximum power peaks occurring at

approximately 18.5 inches below the top of the core in MTR fuel element locations L-25 and L-45. The extrapolated peaking factor at these locations which represents the local power to the core average was found to be 2.5. L-24, L-26, L-44 and L-46 are shim rod locations and these were measured to have maximum-to-core average power ratios of 2.4, occurring approximately 12.5 inches below the top of the fuel in the shim rod. Analysis of the experiment showed the total power produced by element L-25 to be 4.77% of the total reactor power. An energy balance from predictions using the MACABRE-I1 code,[16] which yields slightly conservative results, showed that 4.89% of the reactor power was produced in element L-25.[17] The highest power elements and peaking factors will be used in the thermal hydraulics analysis to determine the allowable operating power level for the Phoenix Fuel core in the MTR.

VII. SHIM ROD STRENGTH AND CALIBRATION MEASUREMENTS

As part of the experimental program, calibration of one interior and one peripheral shim was performed in the PRCF-Phoenix core to determine their incremental worths in reactivity. This calibration was accomplished by incrementally inserting the interior shim (X-4) from 63.6% to 38.9% while incrementally withdrawing the peripheral shim (Z-8) from 0% to 100%. The six remaining shims were banked at 63.6% throughout this calibration measurement. A comprehensive analysis of the peripheral shim calibration has been made and the experimentally determined differential reactivity worths are shown as a function of Q/% versus % withdrawal in Figure 26. These results indicate that the maximum integrated worth of this peripheral shim is (8.27 ± 0.35)$. The criterion used in the selection of the data for this analysis was the requirement that the same operational procedures had to be observed for each period measurement. Each recorded doubling time was then taken to be an independent observation, and these data were then evaluated by computing the reactivity worth at each equivalent power level. Each measured worth reported herein is an average of the differences in reactivity obtained between two successive period runs.

Examination of the differential worth measurements for the peripheral shim over the range of 0% to 90% withdrawn indicated that these data could be fitted with a skewed Gaussian function. The last 10% withdrawal, from 90% to 100%, exhibited a reversal of worth, and this portion of the shim rod calibration curve was extrapolated through to the last 2% withdrawn (98 to 100%). The magnitude of this loss of reactivity was observed to be equal to -(9.6 ± 0.4)¢/% at 99% withdrawn. This phenomenon is believed to result from moving the lower end of the fuel follower out of

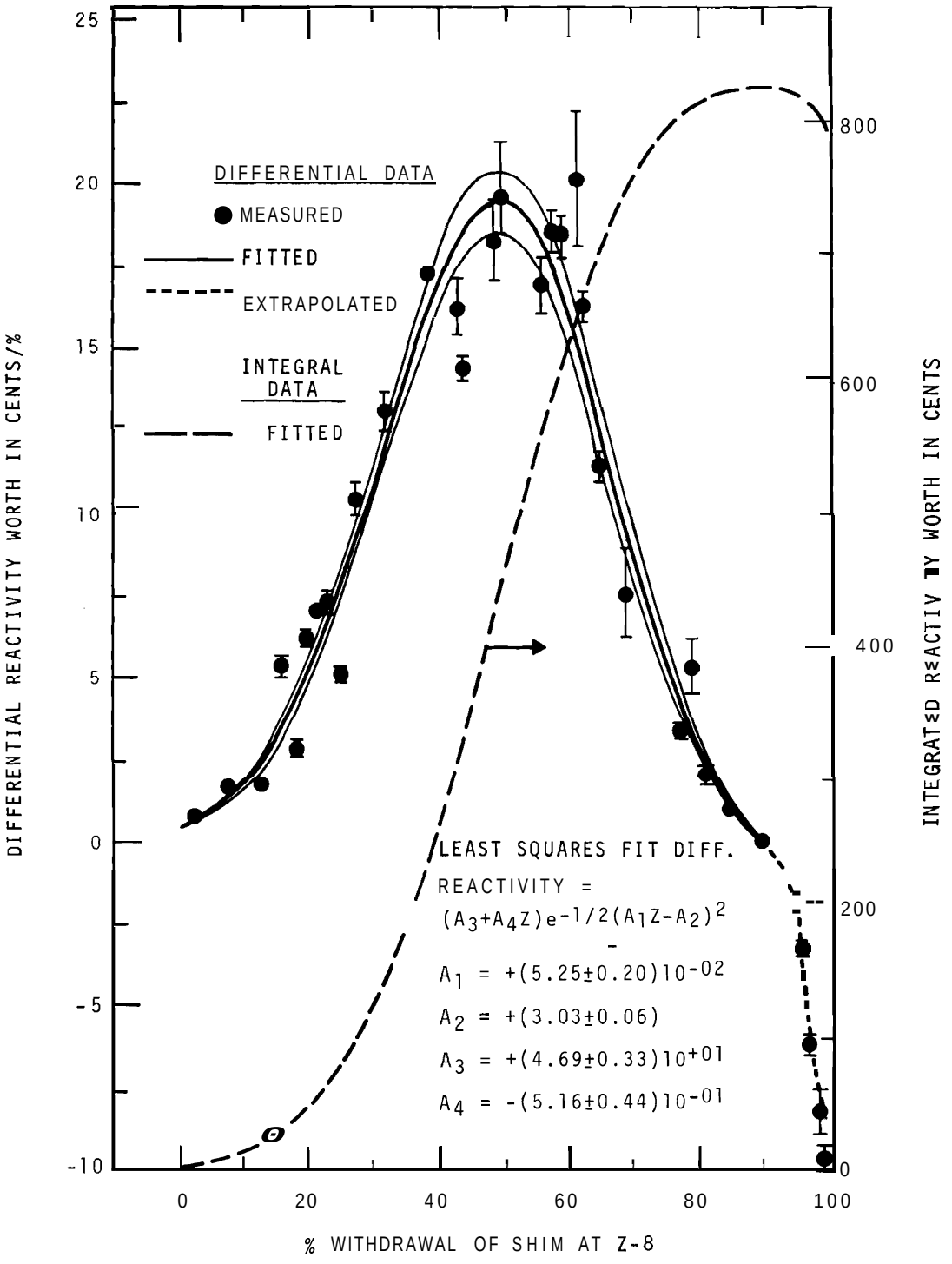

FIGURE 26. Peripheral Shim Rod Calibration in Position Z-8

the region of high thermal neutron flux just below the core, while the upper part of the fuel follower is being moved into the region at the top of the core where the flux is severely depressed by the banked shims. The shim rod calibration measurements were then evaluated using a new subroutine written for the computer code LEARN,[18, 19] which performs a least squares fit to the experimental data using a sum of Hermite polynomials.[20] A best fit to the measured shim data was obtained by applying higher orders of the Hermite polynomial that included the first, second, and fourth terms (n = 0, 1, 3 order) in this analysis. The final results obtained from this analysis are listed in Table V for selected positions on the shim that were also measured.

The second order (n = 2) was not used in this analysis because the squared term would have dominated with a reduction in the magnitude of the central peak and an increase over the remainder of the fitted curve. The measured data did not show these effects, so it was determined that the analysis should be conducted with the zeroth, first, and third order polynomials. The zeroth order Hermite polynomial is a symmetric Gaussian function, and the results of this fit indicated that the function does not satisfactorily meet the requirements imposed by the skewed measured distribution. The first and third order Hermite polynomials met this requirement, but the third order had to be dropped due to the very large error function associated with this fit. The magnitude of these errors over the central region of this third order fit can be observed from the values listed in Table V.

Correlations of the measured variance of the fit* were used to determine that a first order Hermite polynomial should be

---

* *The "measured variance of the fit" is in regard to skewness and variation in the error function for the measured and fitted differential reactivity worths.*

TABLE V. Shim Rod Differential Reactivity Worths in Cents/Percent

% Withdrawal of Shim	Measured	Hermite Polynomials 0th Order	1st Order	3rd Order
2.5	0.83 ± 0.07	0.52 ± 0.09	0.69 ± 0.10	0.70 ± 0.15
21.0	7.03 ± 0.13	5.75 ± 0.37	5.65 ± 0.29	5.62 ± 0.36
38.3	17.35 ± 0.20	17.06 ± 0.81	16.19 ± 0.75	15.91 ± 1.42
49.5	19.67 ± 1.57	19.02 ± 1.12	19.51 ± 0.94	19.67 ± 3.05
61.6	16.35 ± 0.43	12.67 ± 0.85	14.87 ± 0.89	15.50 ± 4.34
75.0	5.26 ± 0.18	4.02 ± 0.38	5.15 ± 0.51	5.33 ± 0.72
89.5	0.18 ± 0.04	0.61 ± 0.10	0.19 ± 0.17	0.17 ± 0.33

utilized. For example, the measured shim rod reactivity worth at 49.5% withdrawn had a recorded uncertainty of ±8%, while the fitted curve value had a computed uncertainty of ±5%. The analytic function that best describes this fit is given as

$$\text{Differential Reactivity Worth} = \left[A_3 + A_4 Z\right] e^{-1/2\,(A_1 Z - A_2)^2}$$

Where

$$A_1 = + (5.25 \pm 0.20) \times 10^{-2}$$

$$A_2 = + (3.03 \pm 0.06)$$

$$A_3 = + (4.69 \pm 0.33) \times 10^{+1}$$

$$A_4 = - (5.16 \pm 0.44) \times 10^{-1}$$

and

Z is the % of shim withdrawn.

The fitted first order Hermite polynomial was integrated by Simpson's Method[21] to obtain the total worth of (8.27 ± 0.35) $ for this peripheral shim (also shown in Figure 26) over the range of 0% to 90% withdrawn. The integrated curve as well as the

error functions of the fit to the polynomial were used to obtain values of the reactivity worth of differential shim movements for interpretation of other experimental measurements.

Eight measured points taken from the calibration of an interior shim in position X-4 were then compared with similar points taken from the fitted shim rod calibration curve. The ratio of the interior shim worth to the peripheral shim worth at each point was found to be 2 (within the uncertainties of the measurements) resulting in a value of (16.54 ± 0.86)$ for the total worth of the interior shim. The total shim rod worth of this core is estimated to be (99.2 ± 3.7)$ or (220 ± 8) mk. The critical loading for this core was achieved with the eight shim rods banked at 59% withdrawn or 3/4 of the total reactivity worth. Therefore, it is estimated that with all eight shims fully inserted, k-effective for this assembly was (0.835 ± 0.006). Measurements of the shutdown margin of the shim rods were conducted at the PRCF for this core. With all interior shims (X-4, X-6, Z-4, Z-6) fully withdrawn, the reactor was estimated to be 3$ subcritical. However, withdrawal of two peripheral and two interior shims on the same end of the core (X-6, X-8, Z-6, Z-8) would have produced a critical core with an estimated excess reactivity of <50¢.

A. ADDITIONAL SHIM CALIBRATION MEASUREMENTS

An experiment was conducted with the standard shimmed core to determine the worth of an additional fuel plate in the shim fuel follower. A new shim fuel follower which was constructed to hold 13 plates replaced the 12-plate follower in the shim at position Z-8 in the core. This shim was withdrawn to 90% to put most of the fuel follower in the active region of the core. The shim in position X-4 was located at 36.4%, and the remainder of the shim rods were positioned at 59% withdrawn. The increase

in the worth of the shim fuel follower due to the addition of the 13th plate was measured to be (26.5 ± 1.3)¢. As a direct result of this experiment, all of the MTR-Phoenix shim fuel followers were designed to contain 13 plates.

A shim calibration point measured in the poisoned core (which had been poisoned to simulate partial xenon poisoning) was compared with a similar point measured in the unpoisoned core. The two values agreed within the uncertainties of the measurements, implying that the shim rod strength will be essentially the same in both the clean and xenon-poisoned cores. Also, a comparison has been made between shim worths measured at elevated temperatures and at room temperature to determine if the fitted shim calibration curve is valid at high temperatures. The results of this analysis, given in Table VI, indicate that the fitted shim calibration curve is valid, within the uncertainties of the measurements, for temperatures up to 52 °C.

TABLE VI. Shim Calibration Measurements at Elevated Temperature

% Withdrawal of Shim	Temperature, °C	Measured Value, ¢/%	Fitted Value, ¢/% (Temp. Range, 28 to 30 °C)
58.6	47.3	16.6 ± 3.9	16.7 ± 0.9
59.4	51.7	15.4 ± 2.7	16.3 ± 0.9

VIII. SIMULATED MTR REGULATING ROD

Measurements were made to determine the reactivity worth of a simulated MTR regulating rod. The mockup of the regulating rod was inserted into Hole No. 1 as shown in Figure 1. A cross section of the reactor extending through the rod mockup in Hole No. 1 is also shown in Figure 3. This regulating rod was constructed by double wrapping a hollow aluminum cylinder with 0.020 inch thick cadmium sheeting over an effective length of 21-1/4 inches. There were no end caps on this hollow tube, and the 7-11/16 inch extender on the bottom of the mockup was perforated. This design allowed the interior of the tube to fill with H_2O to the same height as recorded for the moderator level within the reactor tank. A vertical traversing mechanism was used to incrementally insert or withdraw the rod mockup over its entire stroke of 22 inches. The normal operating range of the MTR regulating rod was established to be equivalent to the upper half of the available stroke in the PRCF (that is, from 11 inches withdrawn to full out).

The total worth over the full stroke of this regulating rod mockup was measured to be (6.1 ± 0.2)¢ in the normal shimmed core and (5.7 ± 0.2)¢ in the partially poisoned xenon core. These reactivity worths were deduced from positive period measurements. The reactivity worth of the simulated regulating rod over the normal MTR operating range was determined to be (1.7 + 1.4)¢. Calculations indicate that translation of the rod from the position of the measurement in the PRCF to the actual MTR location in the reflector, which is 2 inches closer to the center of the core, would increase the worth by a factor of 1.8. Measurements with the regulating rod mockup at a point approximately 6 inches further out from Hole No. 1 in the reflector produced no detectable reactivity change other than a value of (0.5 ± 0.5)¢ obtained for the total worth of this rod.

IX. TEMPERATURE COEFFICIENTS OF REACTIVITY

Measurements of reactivity changes associated with changes in the temperature of the moderator were also made as part of the experimental program over the range of temperatures from 29.1 °C to 57.8 °C. The initial measurement was conducted at room temperature, and then the moderator was heated before each successive measurement. The H_2O in the reactor tank was transferred to a holding tank which was insulated and equipped with special heating coils. Immediately following the period of heating, the H_2O was transferred back to the reactor tank and the period measurements were obtained at this elevated temperature. This procedure was repeated until the final temperature of 57.8 °C was obtained. The same criterion used in the analysis of the shim rod calibration measurements (Section VI) was also applied in the selection of the data to be used in this analysis. This requirement dictated that the same operational procedure be observed for all period runs within this study in order for the resultant reactivity data to be valid. Each recorded doubling time was then taken to be an independent observation, and the data was evaluated by simultaneously comparing the differential results of two successive period runs.

The data obtained from these measurements at elevated temperatures are presented graphically in Figure 27. This figure also illustrates the general trend of the temperature coefficient versus temperature for the PRCF-Phoenix core. The dashed line indicates the calculated profile for the fitted temperature coefficient and its error function over this range of temperatures. These data were calculated by performing a least squares fit to the measured results using a polynomial function within the computer code LEARN.[18, 19] Two requirements were placed on this fit to the measured data. It was

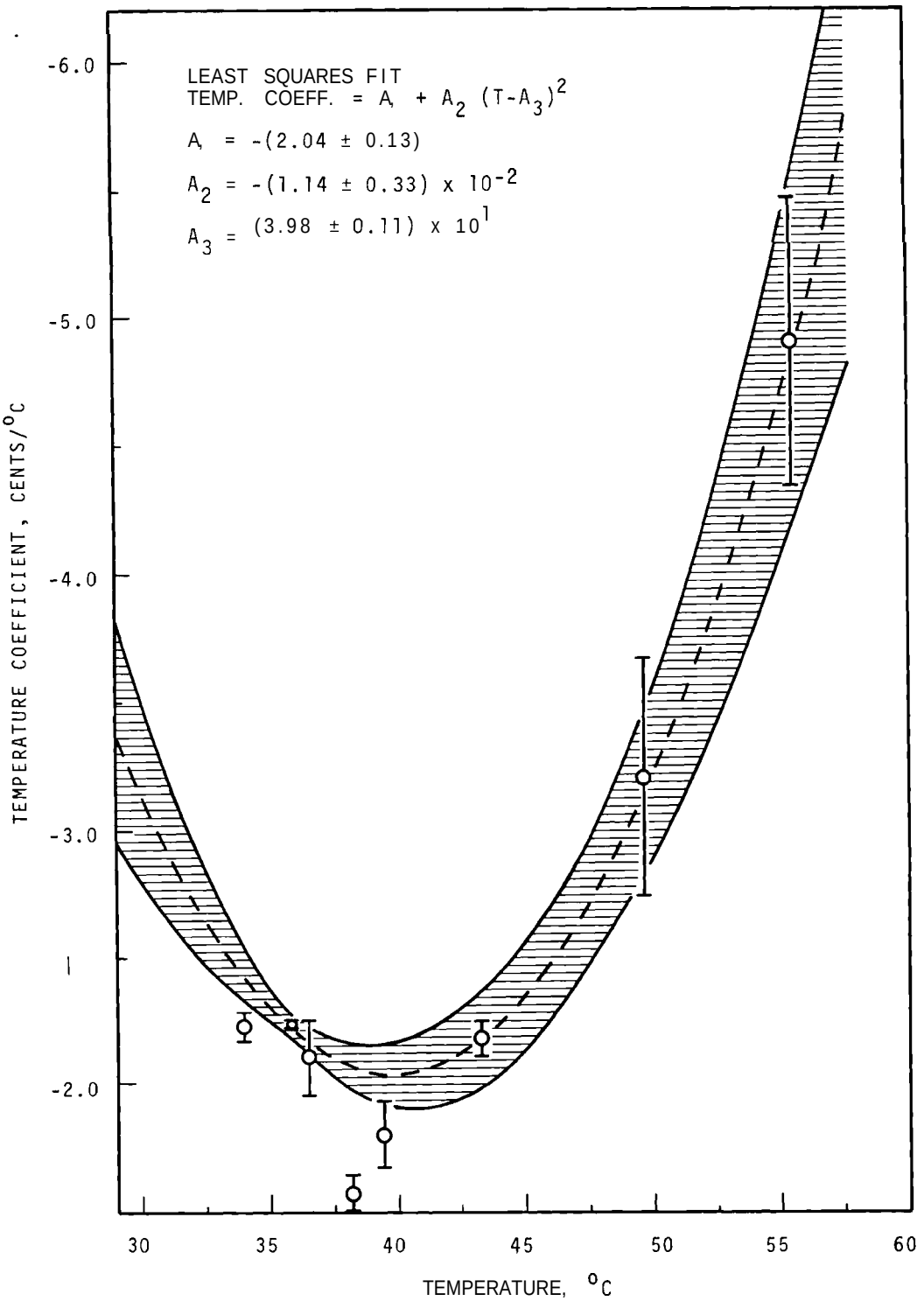

FIGURE 27. Temperature Coefficient Versus Temperature for the Phoenix-Fueled Mockup of the MTR at the PRCF

observed that a minimum must be obtained by the fitted data in the range of temperatures from 34 to 44 °C. Also, the measured values obtained at high temperatures must be described accurately by this fit and its error function in order to interpolate the measured data at the range of temperatures expected during the operation of the MTR. The equation which was used to fit the experimental data to obtain the temperature coefficient as a function of temperature is described by a parabola of the form

$$\text{Temperature Coefficient} = \left[A_1 + A_2 \, (T-A_3)^2\right]$$

where

$$A_1 = -(2.04 \pm 0.13)$$

$$A_2 = -(1.14 \pm 0.33) \times 10^{-2}$$

$$A_3 = (3.98 \pm 0.11) \times 10^{1}$$

and

T is the temperature of the core in °C.

The error function for the fitted temperature coefficient was programmed, and values of the errors for the fitted curve were evaluated for various temperatures. The results of this analysis indicate that the magnitudes of the uncertainties on the fitted data are consistent with the uncertainties of the measured data. For example, the measured temperature coefficient at 49.7 °C was determined to be uncertain by ±14%, while the fitted curve value at this temperature had a computed uncertainty of ±10%. The measured data points are compared with the results obtained from the fitted function in Table VII. The temperature coefficient of reactivity for this core is negative for all values of temperature and is increasingly negative at higher temperatures.

TABLE VII. PRCF – Phoenix Core Temperature Coefficients of Reactivity

Temperature, °C	Measured, ¢/°C	Fitted, ¢/°C
35.89	-(2.24 ± 0.02)	-(2.21 ± 0.04)
36.49	-(2.10 ± 0.15)	-(2.16 ± 0.05)
39.82	———	-(2.04 ± 0.13)
43.27	-(2.18 ± 0.07)	-(2.17 ± 0.18)
49.72	-(3.21 ± 0.46)	-(3.16 ± 0.32)
55.45	-(4.91 ± 0.56)	-(4.84 ± 0.68)

X. LOSS OF COOLANT MEASUREMENTS

An extensive series of measurements were made in the shimmed core to determine the reactivity changes which could be associated with loss of coolant from the core. H_2O coolant was excluded from selected coolant channels in various positions of the core by inserting aluminum or Teflon strips into the elements. A special upper end box was designed and adapted to fit one of the stationary fuel assemblies after removing the original end box. This design change allowed the strips to be withdrawn or inserted without removing the element from the core. When the set of measurements in a particular core lattice location were terminated, the special element would be moved to another position within the core. Some of the measurements required only that positive periods be obtained while others also required shim movements as well. The final data obtained from this experiment and reported herein are the results of two or three separate measurements performed at each position within the element. These measurements included the strip being inserted as well as being withdrawn. This procedure was followed until the reactivity map of this core for the voiding experiment was completed. The strips were as long as the fuel plates and were either partial width (0.26 void fraction) or full width (0.8 void fraction). The partial width strips were positioned either at the center of a coolant channel or at the east side of the channel. The average dimensions and percent voids of these aluminum and Teflon strips are listed in Table VIII.

The experimental data obtained from the simulated voids produced by inserting the partial strips into Channel 8 were analyzed and these results are given in Table IX. The insert of the cutaway element within Figure 28 shows how the plates are numbered; thus, Channel 8 of this element would be the channel between Plates 8 and 9.

TABLE VIII. Average Dimensions and Percent Void Simulated by Using Plates of Aluminum and Teflon in the coolant-channels of the PRCF–Phoenix Core

	Aluminum			Teflon		
	Thickness, in.	Width, in.	% Void Single Channel	Thickness, in.	Width, in.	% Void Single Channel
Partial Channel Voiding	0.094	0.870	26.2	0.095	0.869	26.4
Single Full Channel Void	0.094	2.554	76.8	0.095	2.557	77.7
Multiple Full Channel Voids	0.094	2.571	77.3	—	—	—

TABLE IX. Reactivity Worth of Simulated 26% Coolant Void in Channel No. 8

Element Location	X-1	X-5	Y-5	Y-5
Position in Channel	East Side	East Side	East Side	Center
Reactivity Change on Voiding by:				
Aluminum	-(0.5 ± 0.3)¢	-(7.9 ± 0.3)¢	-(9.2 ± 0.5)¢	-(13.9 ± 1.4)¢
Teflon	-(0.9 ± 0.2)¢	-(6.9 ± 0.2)¢	-(11.2 ± 0.5)¢	—

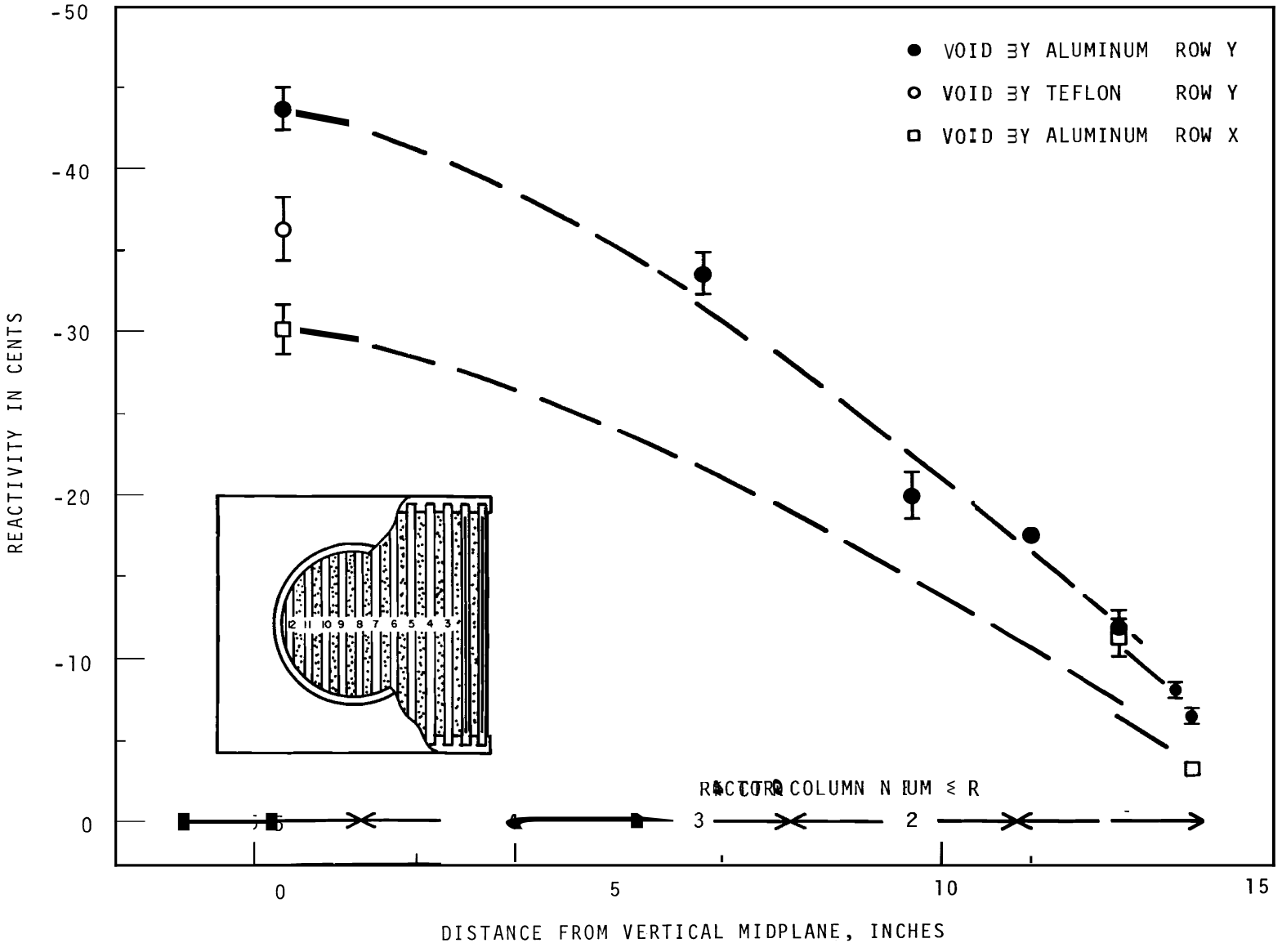

FIGURE 28. Reactivity Worth of ∿0.8 Voids Simulated by Aluminum and Teflon

The results which were obtained for the partial aluminum strip that was inserted into the element in position Y-5 were accumulated from the data in Table IX using core symmetry arguments to generate an equivalent full channel value. The full-channel strip measurement, made in that same core position, was then compared with this accumulated value to determine the interaction of the partial strips. The partial strip values added up to -(32.3 ± 1.6)¢ worth in reactivity which was equivalent to a channel voiding of 78.6%. The full channel measurement essentially occupied the same volume (76.8% void) as the accumulated partial strips, but this result was recorded to be -(43.7 ± 1.2)¢ or 35% larger in magnitude. All of the measured results obtained from simulating an 80% void with aluminum or Teflon are illustrated graphically in Figure 28. The curves presented herein are estimated profiles of the voiding worth due to inserting aluminum strips into rows X and Y. These results indicate that there is a 30% decrease in the reactivity worth from row Y to X for the same channel location at the center of the core. There is a 50% decrease in the measured worth from row Y to X at the edge of the core in Channel 1. In addition, the void result produced by the Teflon which was inserted into Channel 8 of the element in core location Y-5 is roughly 80% of the value measured for aluminum. The results of these measurements can be summarized in general as follows: the reactivity changes due to loss of H_2O coolant were always negative, small near core edges, and larger in the core interior with the maximum at the center.

A. OTHER SELECTED VOIDING MEASUREMENTS

In addition to the previously discussed void measurements, multiple-channel void worths were measured at the center of the core in Channel 8 of fuel position X-5, Y-5, and Z-5. This

measurement was performed by a differential movement of the shim at core location Z-8 from a base of 42.5% to 46.3% withdrawn after loading aluminum strips into the stationary elements. The worth of this central core void was determined to be -(0.97 ± 0.04)$. The results which were obtained for the full width aluminum strips inserted into the elements in position X-5 and Y-5 were accumulated from Figure 28 to generate an equivalent multiple channel value for comparison. Using core symmetry arguments, these full strips add up to -(1.04 ± 0.03)$ worth in reactivity for a void equivalence of 76.8%. The multiple-channel void measurement occupied a volume that is essentially the same, and Table VII shows this to be a 77.3% void. These results indicate that, in reality, the interaction of these aluminum strips probably cannot be detected within the uncertainties to be associated with the equivalent value of ∿1.04$ that was generated.

This experiment for determination of the reactivity worths of multiple channel voids was continued by voiding six more channels with additional aluminum strips. The strips were loaded into Channels 7 and 9 in-the same three elements. The worth of the three to nine aluminum-plate addition was determined to be -(1.71 ± 0.08)$ by another differential shim movement from 46.3% to 55.5% withdrawn. The accumulation of both these results (that is, zero to three plates plus three to nine plates) yields an equivalent nine-plate void of -(2.68 ± 0.09)$ worth in reactivity. This compares very favorably with the measurement obtained with all simulated voids removed, and the shim at Z-8 returned to the original base of 42.5%. The resultant worth of this nine-channel void measurement was determined to be -(2.77 ± 0.09)$.

XI. LOSS OF FUEL PLATES

Measurements were made to determine the reactivity worth of the remcval of a whole element from the center cf the core (Y-5), of single plates from an element at the center of the core (Y-5), and of a plate at the side of the core (X-5). The 16 plates in a stationary fuel element are numbered sequentially through 16 as shown in Figure 28. The order of plate removal from core lattice position Y-5 was such as to maintain symmetry around the center line of the element. Five of the central plates from this element were sequentially removed one at a time, and then all five plates were simultaneously replaced. Some of these measurements required only positive periods be performed while others also required shim movements. One of these measurements was obtained by subcritical extrapolation of the multiplication data generated upon withdrawing all the sheets and observing that the reactor was still subcritical. This particular measurement was repeated twice to ensure the validity of the observed effect on magnitude and sign of the resultant reactivity worth to be associated with this plate removal. The reactivity change is highly positive for the first plate removed and requires the removal of a total of four plates before the differential worth reverses its sign. The final data obtained from this experiment for the shim positions as well as the resultant reactivity worths of the plate removals are listed in Table X.

The accumulated reactivity worth of sequentially removing the five central plates was determined by adding up the values listed in Table X to obtain +(56 ± 3)¢. This value compares favorably with the measured reactivity worth of +(62 ± 4)¢ that would be obtained upon removing the five plates simultaneously. This measured value was inferred from the result that was obtained by replacing the five plates and returning

TABLE X. Reactivity Worth of Plates Removed from the Element in Core Lattice Position Y-5

Order of Removal	Plate Number	Method of Measurement	Shim Movement, % Withdrawal	Reactivity Worth, ¢
1	8	Positive Period to Sub-critical Extrapolation	35.9	42.2 ± 1.9
2	9	Positive Periods	34.0	15.6 ± 1.6
3	7	Positive Periods and Shim Measurement	34.0 to 32.2	18.8 ± 1.5
4	10	Positive Periods and Shim Measurement	32.2 to 31.6	-0.7 ± 0.2
5	6	Positive Periods and Shim Measurement	31.6 to 32.7	-20.0 ± 1.0

the shim at Z-8 from 32.7% to 37.2% withdrawn. In addition to these measurements, a plate was removed from Position 8 of X-5, and the effect was observed to be +(24.3 ± 1.4)¢ or about half as large as the worth of the corresponding plate removed from Y-5. The total worth of the most central fuel element in core lattice position Y-5 was inferred by measurement to be equal to (5.92 ± 0.27)$. This measured value was obtained upon inserting this element back into the core after completing the reactor noise measurements. The shim at Z-8 was initially located at 85% withdrawn and it had to be moved a total span of 47.5% to 37.5% withdrawn to compensate for the reactivity insertion.

Calculations[22] were also performed to simulate the effects caused by removal of the individual fuel plates from the element in Y-5. These calculations were performed using a four-energy group diffusion theory representation of the reaction in slab geometry. Successive valves of k_{eff} were calculated for six cases, and these were used to obtain incremental worths for each plate removed from zero to five plates. The worth curves for

both the experiment and calculation have been generated by interconnecting the results obtained by straight lines. These curves are illustrated in Figure 29. The calculation not only indicates a highly positive reactivity change to be associated with the removal of the first fuel plate, but the shape of this curve is similar to that of the experiment as well. The incremental worths are greater for the calculational model than the experimental results since the zone used to simulate the plates being removed extended completely across the core. In addition, the calculation required a total of four and one-fourth plates to be removed, as compared to the four plates for the experiment, before the differential worth reversed its sign. It can be concluded from this information that the analytical model employed in this calculation did a favorable job in predicting the experimental effects noted for the removal of the fuel plates from the center of the core.

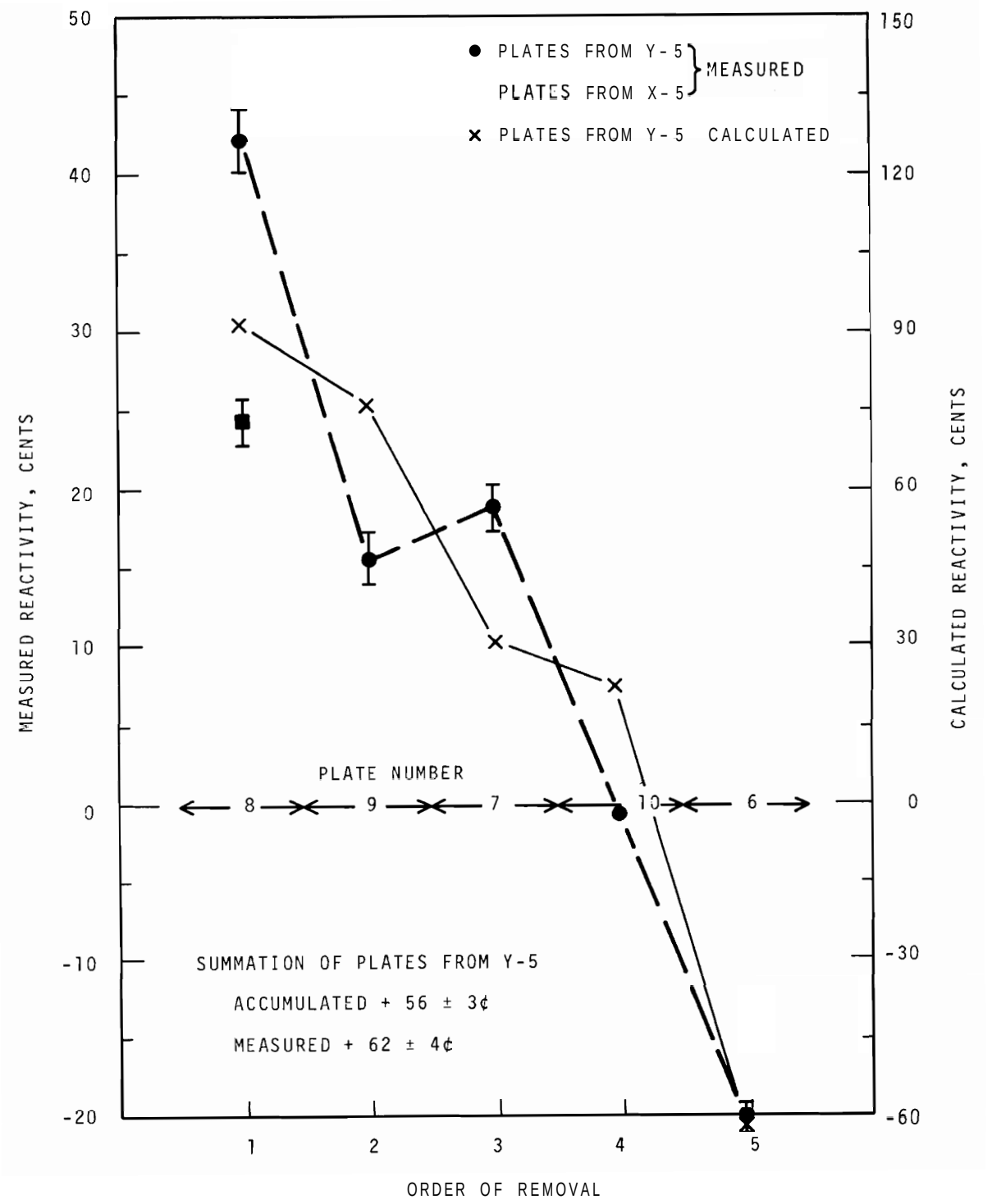

FIGURE 29. Measured and Calculated Reactivity Worth of Fuel Plate Removal from the PRCF–Phoenix Fuel Core

XII. REACTOR NOISE MEASUREMENTS

Reactor noise data were recorded in the PRCF-Phoenix core by use of five detectors located in three typical positions: (1) center of the core, (2) beryllium reflector, and (3) H_2O top reflector. One BF_3 detector was loaded into a dummy element, and this assembly was inserted into the reactor lattice position Y-5. Two BF_3 chambers were positioned on top of the beryllium reflector at the North and South edges of the fuel core. Two additional BF_3 detectors were placed into Hole No. 1 in the beryllium reflector. The chamber locations in the reactor where noise data were successfully measured are diagrammed schematically in Figure 30. No interpretable results were obtained from the chambers in the H_2O top reflector. Satisfactory results were obtained from the chambers in the beryllium reflector and in the center of the core with the critical height of the banked shims at 63.5% withdrawn. The final results obtained from the analysis of these recordings for β/ℓ, the effective delayed neutron fraction divided by the prompt neutron lifetime, are listed in Table XI.

TABLE XI. PRCF–Phoenix Fuel Reactor Noise Analysis

	Core Center	Beryllium Reflector
β/ℓ, sec^{-1}	59.4 ± 0.7	59.9 ± 1.0

The quantity usually obtained from experimental noise measurements is the power spectral density, and from this, one deduces the kinetic parameters of the reactor. Experimentally, the power spectral density is obtained by recording and analyzing a signal which is proportional to the statistical fluctuation of the neutron population about some average value. This fluctuation is reactor noise.[23]

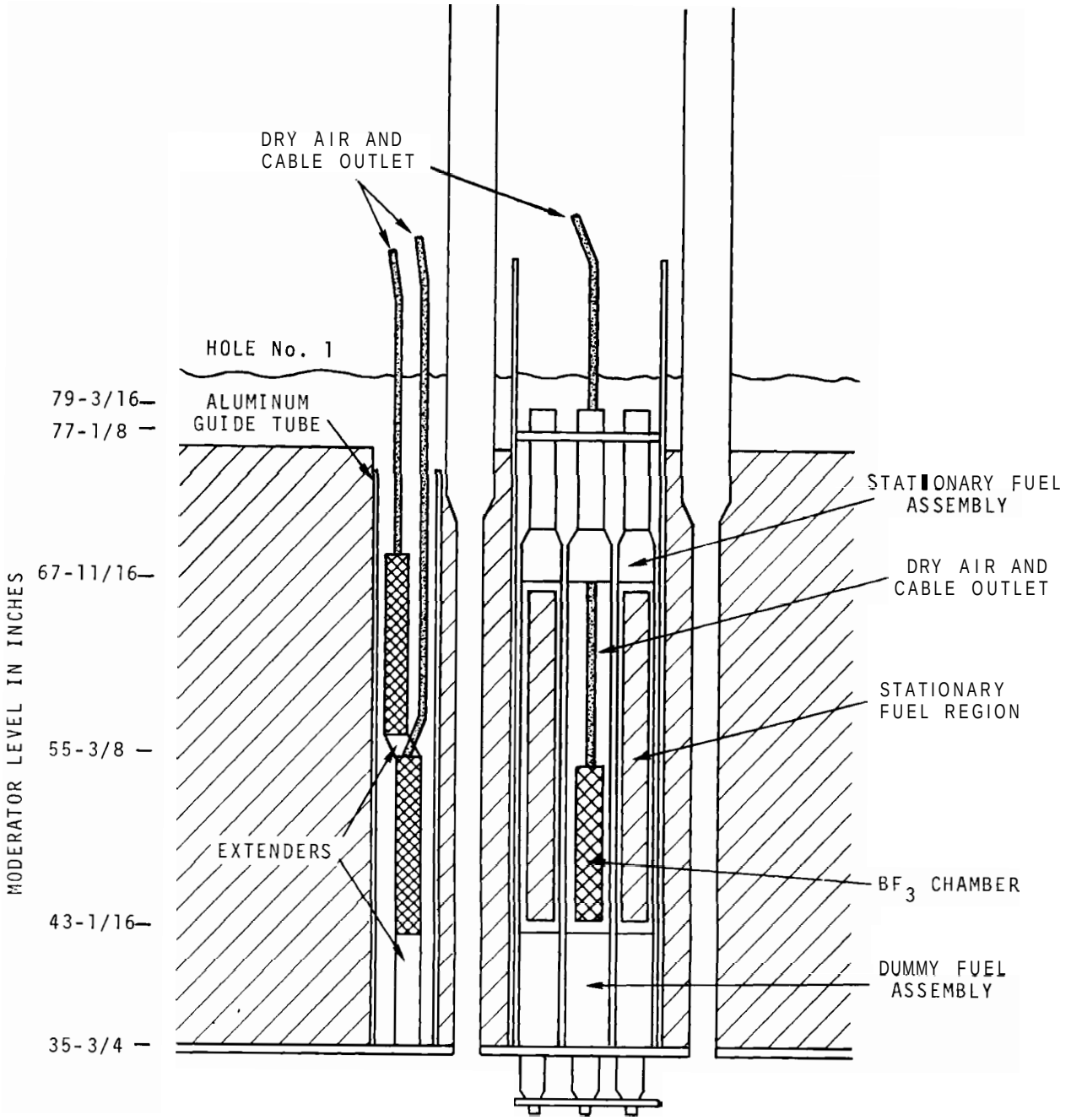

FIGURE 30. Locations of BF_3 Chambers Utilized in the β/ℓ Determination at the PRCF Mockup of the MTR–Phoenix Fuel Core

Analytically, this quantity can be derived from the space-independent form of the neutron kinetics equations.[24] Using the approximation of one delayed group of neutrons,[25] the power spectral density can be expressed as

$$|n(\omega)|^2 = |TF|^2 = \left(\frac{n_o}{\ell\omega}\right)^2 \frac{(\omega^2 + \bar{\lambda}^2)}{(\omega^2 + \alpha^2)} + N$$

where

$n(\omega)$ = neutron flux as a function of frequency

TF = transfer function

n_o = initial value of neutron flux

ω = frequency

$\bar{\lambda}$ = the mean decay constant of the delayed neutron precursors

$\alpha = \beta_{eff}/\ell$

N is a background term that is independent of frequency.

In the analysis of noise data, one infers the reactor kinetic parameters from the shape of the power spectral density as a function of frequency. The following form of equation was used to fit the measured power spectrum data points (that is, power per unit band width):

$$y = A_1 + \frac{A_2}{\omega^2} \frac{\left(A_3^2 + \omega^2\right)}{\left(A_4^2 + \omega^2\right)}$$

where

$A_1 = N$

$A_2 \alpha (n_o/\ell)^2$

$A_3 = \bar{\lambda}$

$A_4 = (\beta_{eff}/\ell)$

This equation has been further modified as follows:

(1) It was multiplied by a term, $\frac{(A_5)^2}{\omega^2 + (A_5)^2}$,

that represents the ionization chamber response. This term is required whenever the break frequency (β/ℓ) occurs at a frequency high enough to be interfered with by the response of the system.

(2) One term was treated as zero, neglecting the parameter A_3 which in this analysis is not physically significant since it contains effects of extraneous low frequency signals. This treatment of A_3 simplifies the theory and does not affect the results in the frequency range of interest (that is, near $\omega = \beta/\ell$).

The final form of the equation used in this analysis was

$$y = \left\{\hat{A}_3 + \left[\frac{\hat{A}_2}{(\omega^2 + \hat{A}_2)}\right]\hat{A}_1\right\}\left\{\frac{\hat{A}_4}{(\omega^2 + \hat{A}_4)}\right\}$$

and one can obtain this equation by performing the following substitutions:

Let

$$\hat{A}_4 = A_5^2,\ \hat{A}_3 = A_1,\ \hat{A}_2 = A_4^2,\ \text{and}\ \hat{A}_1 = A_2/A_4^2.$$

This fitting of the measured data points was accomplished using Program NOISE[25,26] which uses the general least squares techniques incorporated in the computer code LEARN.[18,19] The fitting procedure incorporates nonlinear iterative logic and statistics which involve both first- and second-order differentials. The fitting procedure yields values for all the parameters involved, together with their errors. The frequency plots obtained from this analysis are reproduced in Figures 31 and 32. Analysis of the data from the chamber in the beryllium reflector produced results not significantly different from the chamber located at the center of the core.

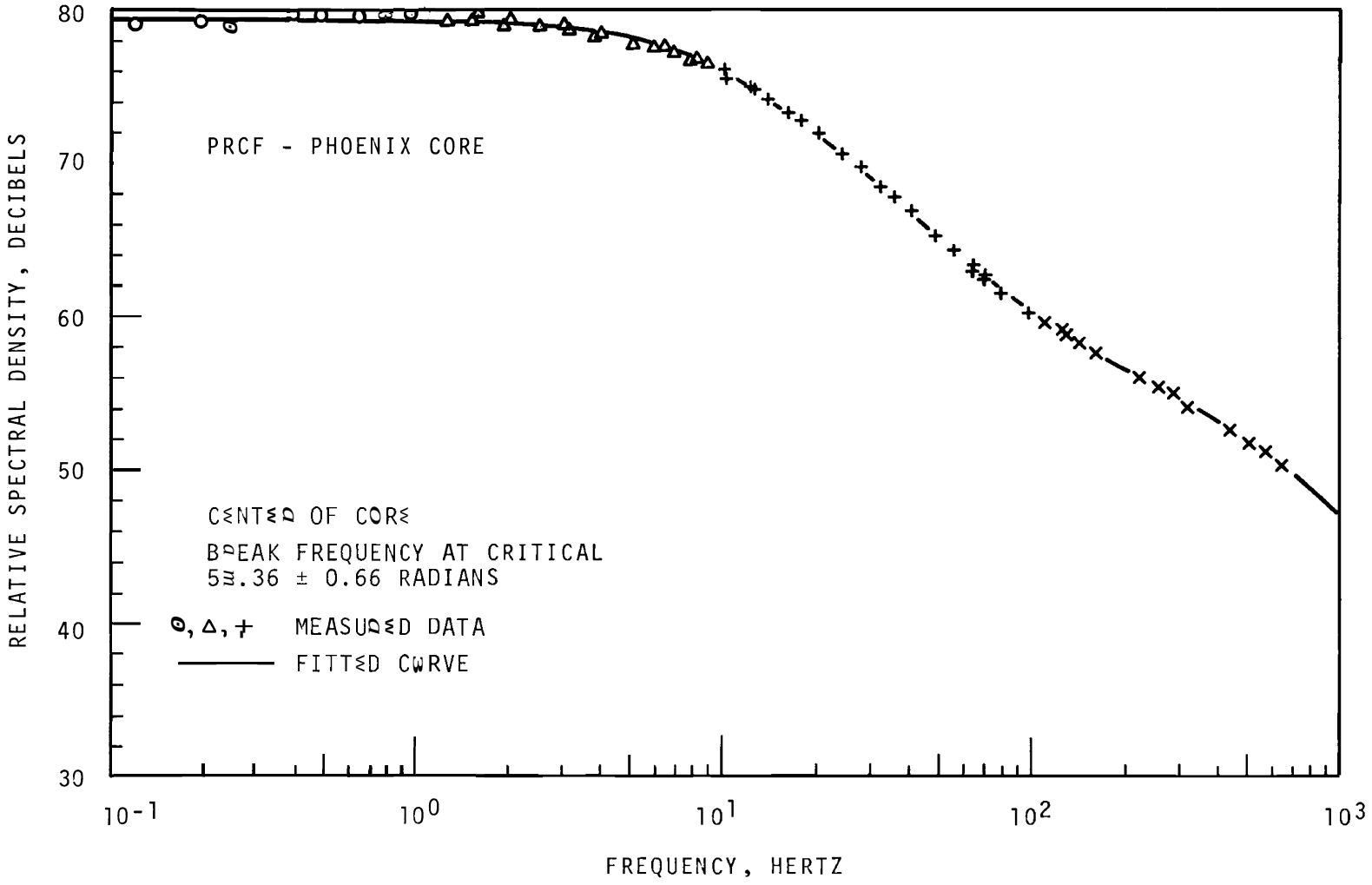

FIGURE 31. Spectral Density for PRCF-Phoenix Fuel Mockup of the MTR for Chamber Located at Center of the Core

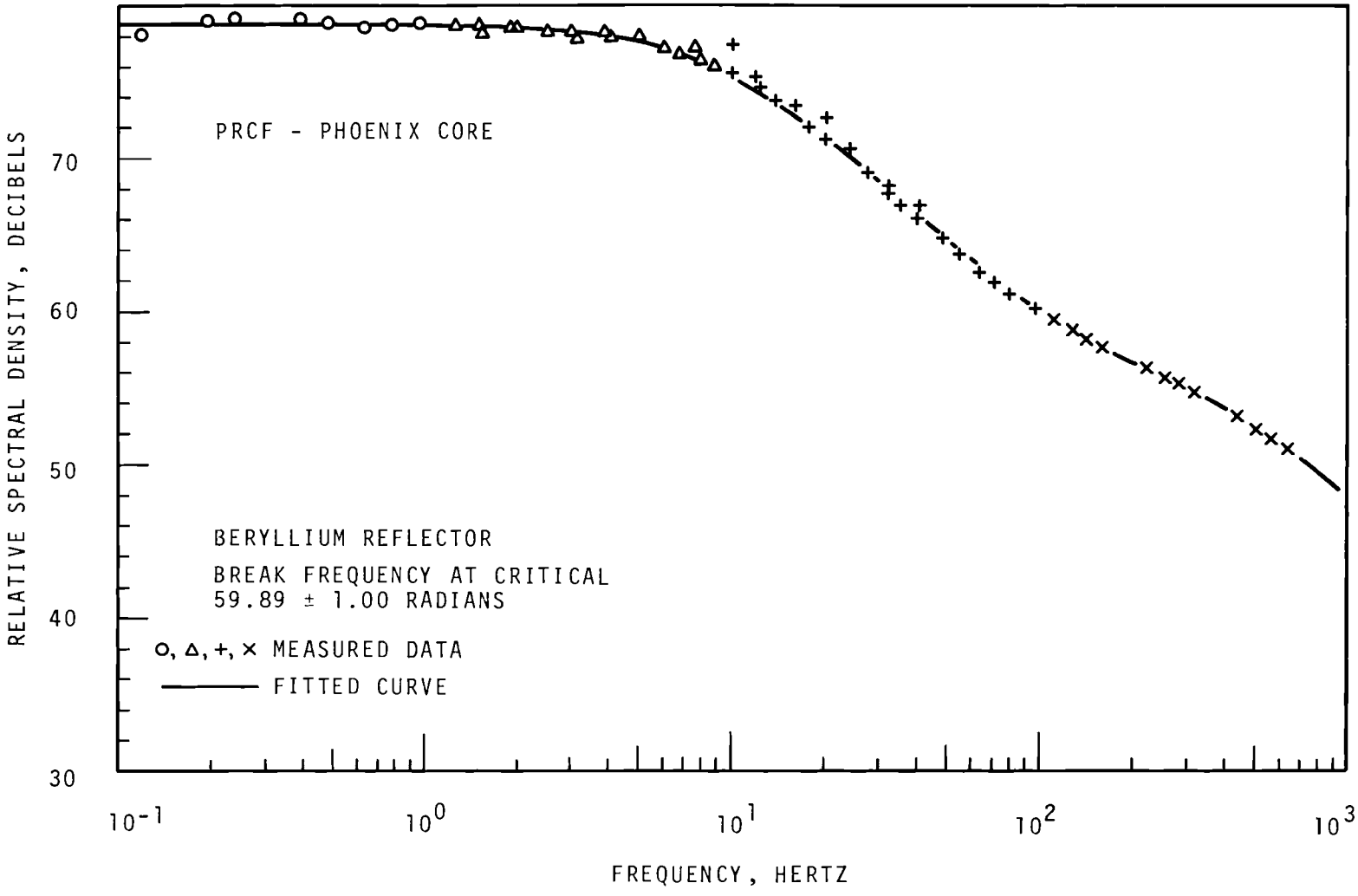

FIGURE 32 Spectral Density for PRCF-Phoenix Fuel Mockup of the MTR for Chambers Located in Hole No. 1 of the Beryllium Reflector

Upon completing the measurements in this core, it was decided that a computation of the kinetic parameters should be performed for comparison. The computer code KINPAR[27] has been used to calculate values of the effective delayed neutron fraction, β_{eff}, and the prompt neutron lifetime, R, for a core composed of this type of fuel.

The KINPAR code is linked to the one-dimensional, multigroup, diffusion-theory code HFN,[15] from which direct and adjoint fluxes are obtained for the perturbation theory expressions. The isotopic delayed neutron fractions used in KINPAR are from Reference 28. Average inverse velocities, prompt neutron spectra, and values of $\overline{\nu\sigma_f}$ were obtained from cell calculations using the computer codes THERMOS/BATTELLE[29] and HRG (Hanford Revised GAM[30]). The average inverse velocity was obtained according to the equation

$$\left(\frac{1}{\bar{V}}\right) = \frac{\int \left(\frac{1}{v}\right) \phi \; dE}{\int \phi \; dE}$$

The code KINPAR uses standard perturbation-theory expressions for the quantities β_{eff} and R.[28] The specific expressions used are:

$$\beta_{eff} = \frac{\sum_{m=1}^{M} \int_v \left[\sum_{j=1}^{J} (\nu \Sigma_f)_j^m \phi_j\right] \cdot \left[\beta^m \cdot \sum_{j=1}^{J} \chi_j^D \phi_j^*\right] dv}{\sum_{m=1}^{M} \int_v \left[\sum_{j=1}^{J} (\nu \Sigma_f)_j^m \phi_j\right] \cdot \left[\beta^m \cdot \sum_{j=1}^{J} \chi_j^D \phi_j^* + (1-\beta^m) \cdot \sum_{j=1}^{J} \chi_j^p \phi_j^*\right] dv}$$

and

$$\ell = \frac{\int_v \sum_{j=1}^{J} \left(\frac{\phi_j^* \phi_j}{V_j} \right) dv}{\sum_{m=1}^{M} \int_v \left[\sum_{j=1}^{J} (\nu \Sigma_f)_j^m \phi_j \right] \left[\sum_{j=1}^{J} \chi_j^p \phi_j^* \right] dv}$$

where

β_{eff} = total effective delayed neutron fraction

M = total number of fissionable species present

$\nu \Sigma_{fj}^m$ = macroscopic nu sigma fission for energy group j for material m

ϕ_j = real flux for energy group j

ϕ_j^* = adjoint flux for energy group j

χ_j^D = fraction of delayed fission neutrons emitted into energy group j

χ_j^p = fraction of prompt fission neutrons emitted into energy group j

β^m = total fraction of delayed fission neutrons emitted by material m

$1/V_j$ = average inverse velocity of neutrons in j energy group

J = number of energy groups for which fluxes are to be calculated

$\int_v$ = integration over volume of entire reactor.

A four-region, 17-energy group calculation of the PRCF-Phoenix core was performed using the KINPAR program. A core of fixed elements with a beryllium and H_2O reflector, in slab geometry, was assumed for this calculation. The group structure and other details of the analytical model are contained in Figure 33.

The KINPAR calculation for this particular type of core loading with stationary fuel assemblies yielded values of $\beta = 2.77 \times 10^{-3}$ and $\ell = 3.38 \times 10^{-5}$ seconds. The ratio for β/ℓ as determined by this computation is 82 sec^{-1}, and this one-dimensional calculation was performed to yield a value of β/ℓ for a check on the order of magnitude to be expected from a measurement. The experimental value of $(59.4 \pm 0.7) sec^{-1}$ for β/ℓ was obtained from a measurement in the 3 × 9 shimmed core. The KINPAR calculation yielded results that are different than the experimental values because of the clean core model chosen for this analysis. The plane selected for this calculation passed only through fixed elements (that is, like X-, Y- and Z-5). This analytical model was necessarily one-dimensional because of the linkage of the KINPAR code to HFN, and the model did not include the shim control rods.

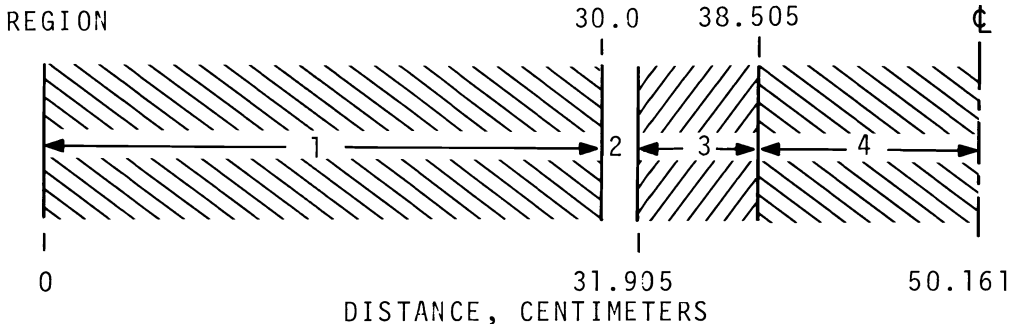

REGION #	COMPOSITION
1.	BERYLLIUM
2.	WATER IN CONTROL SLOT
3.	BERYLLIUM
4.	SLAB CORE

GROUP	UPPER ENERGY, eV
1	10×10^{6}
2	2.23×10^{6}
3	1.05×10^{6}
4	4.98×10^{5}
5	2.35×10^{5}
6	1.11×10^{5}
7	5.25×10^{4}
8	2.48×10^{4}
9	1.17×10^{4}
10	5.53×10^{3}
11	2.61×10^{3}
12	1.23×10^{3}
13	2.75×10^{2}
14	6.14×10^{1}
15	1.37×10^{1}
16	3.06
17	0.683

FIGURE 33. PRCF-Phoenix Core Model Utilized for KINPAR Calculation to Obtain Values of β, ℓ and β/ℓ for Clean Cores

ACKNOWLEDGMENTS

The critical experiments that were conducted in the MTR mockup at the PRCF and the analytical work required to compile, reduce, and analyze the data from these experiments took place over a 2-year period, and many people contributed. Program management was provided by L. C. Schmid, D. D. Lanning, G. J. Busselman, and R. I. Smith. The principle author, E. C. Davis, Jr., had the primary responsibility for conceiving, designing, planning, and directing the efforts as well as accepting the data, analyzing and reporting the physics experiments for the Phoenix Fuel Program.

Reactor operations and gamma scanning assistance was contributed by L. D. Williams, J. B. Edgar, and G. J. Konzek. A. R. Maki, A. E. Penttila, J. E. Choate, and I. N. Sorrells performed general assistance as required in experiment preparation and data acquisition. General data reduction and analytical assistance was provided by E. B. Reppond and T. M. Traver. Analytical assistance and model development for the Phoenix fuel core was contributed by C. M. Heeb and W. W. Porath. D. A. Kottwitz and R. P. Matsen provided the theoretical arguments for and the analytical derivation of the equations and error functions used to fit the shim calibration measurements. G. D. Seybold performed the computer programming required to obtain the least squares fits to the shim calibration and temperature coefficient measurements. The reactor noise analysis for the determination of β/ℓ was conducted by W. P. Stinson.

REFERENCES

R. A. Bennett and L. C. Schmid. Approach-to-Critical and Calibration Experiments in the Plutonium Recycle Critical Facility, HW-80206. Available from Clearinghouse for Federal Scientific and Technical Information, Springfield, Virginia, 1964.

2. G. J. BusseZman. "Phoenix Fuel for Test Reactors," Trans. Am. Nucl. Soc., vol. 10, p. 311. 1967.

3. P. L. hofmann, G. J. BusseZman, and R. H. Holeman. Nuclear Characteristics of Some Compact, Water Moderated Plutonium Burners, HW-79977. Available from Clearinghouse for Federal Scientific and Technical Information, Springfield, a , 1964.

R. H. Holeman and P. L. Hofmann. Nuclear Design Calculations for a Hx-Pu Fueled MTR, HW-84575. Available from Clearinghouse for Federal Scientific and Technical Information, Springfield, Virginia, 1964.

5. D. D. Lanning and G. J. BusseZman, Editors, Phoenix Fuel Program Progress Report, BNWL-635. Battelle-Northwest, RichZand, Washington, November 1967.

6. D. G. Albertson and G. J. BusseZman. "Analysis and Measurements of Pu-Al Polyethylene Systems in the PCTR," Trans. Am. Nucl. Soc., vol. 8, p. 448. 1965.

7. W. P. Stinson and C. M. Heeb. "Approach-to-Critical Experiments with Phoenix Fuel," Trans. Am. Nucl. Soc., vol. 10, p. 187. 1967.

8. R. I. Smith, E. C. Davis, and L. D. Williams. "Critical Experiments with Phoenix Fuel in an MIR Mockup," Trans. Am. Nucl. Soc., vol. 10, p. 537. 1967. E. C. Davis, et al. BNWL-472, 534, 634, 685, 775, 887, 921 and 985, Reactor Physics Quarterly Reports for 1967 and 1968, Battelle-Northwest.

9. C. M. Heeb. Analysis of the Phoenix Fuel Experiments, BNWL-1514. Battelle-Northwest, November 1970.

10. R. G. Curran and R. R. Sharp. "Fabrication of Phoenix MIR Fuel Elements," Trans. Am. Nucl. Soc., vol. 12, p. 97. 1969.

11. R. S. Marsden, R. L. Curtis, and D. W. Knight. Safety Analysis Report for the MTR Phoenix Fuel Experiment, INC-1209. Idaho Nuclear Corporation, 1969.

12. E. E. Burdick and N. C. Paufman. The MTR-Phoenix Fuel Experiment - MTR Startup and Operation, INC-1327. Idaho Nuclear Corporation, 1969.

13. T. B. Fowler, M. L. Tobias, D. R. Vondy. EXTERMINATOR - A Multigroup Code for Solving Neutron Diffusion Equations in One and Two Dimensions, ORNL-TM-842. Oak Ridae Naticnal Laboratory, February 1965.

14. T. B. Fowler and M. L. Tobias. Whirlaway - A Three-Dimensional, Two Group Neutron Diffusion Code for the IBM-7090 Computer, ORNL-3150. Oak Ridge National Laboratory, 1961.

15. J. R. Lilley. Computer Code HFN-Multigroup, Multiregion Neutron Diffusion Theory in One Space Dimension, HW-71545. 1961.

16. M. L. Griebenow and K. D. Richert. MACABRE 11 (User's Manual), IN-1107. Idaho Nuclear corporation, September 1967.

17. R. M. Hiatt. "Thermal Hydraulics of the MTR-Phoenix Core," Reactor Physics Department Technical Activities Quarterly Report, April, May, June, 1968, BNWL-887. Battelle-Northwest, November 1968.

18. B. H. Duane. Maximum LikeZihood Nonlinear CorreZated Fields (BNW Program LIKELY), BNWL-390. Battelle-Northwest, September 1967.

19. G. D. Seybold. User's Aid: Programs LEARN and LIKELY, BNWL-1057. Battelle-Northwest, 1969.

20. Vladimir Rojansky. Introductory Quantum Mechanics. Prentice Hall, Inc., Englewood Cliffs, New Jersey, 1938. p. 23.

21. T. S. Peterson. Elements of Calculus, Harper and Brothers, New York, 1950. p. 207.

22. C. M. Heeb. "Analysis of MTR Mockup Phoenix Fuel Critical Experiments," Reactor Physics Department Technical Activities Quarterly Report, October, November, December 1967, BNWL-685. Battelle-Northwest, March 1968.

23. O. Uotinen, J. H. Lauby, W. P. Stinscn, S. R. Dwivedi. Measured and Calculated β_{eff}/ℓ for Uniform H_2O Luttices of Al-Pu, UO_2, and UO_2-PuO_2 Fuel Rods, BNWL-SA-2688. Battelle-Northwest, 1969.

24. G. R. Keepin. Physics of Nuclear Kinetics. Addiscn-Wes Zey Publishing Co., Reading, Masrachusetts, 1965. p. 282.

25. L. C. Schmid and G. D. Seybold. "Computer Analysis of Reactor Noise Data," Physics Research Quarterly Report, January, February, March 1966, BNWL-284. Battelle-Northwest, April 1966.

26. G. D. Seybold, Unpublished Data. Battelle-Northwest, Rich Zand, Washington, 1966. (Pre Ziminary Report: Program NOISE.)

27. N. E. Carter and W. L. Purcell. Unpublished Data. Battelle-Northwest, Rich Zand, Washington, 1969. (Pre Ziminary Report: KINPAR: A Computer Code to Perform Perturbation Theory Calculation of Effective Delayed Neutron Fractions and Prompt Neutron Lifetime.)

28. Reactor Physics Constants, Second Edition, ANL-5800. Argonne National Laboratory, 1963.

29. D. R. Skeen and L. J. Page. THERMOS/BATTELLE: The Battelle Version of the THERMOS Code, BNWL-516. Battelle-Northwest, September 1967.

30. J. L. Carter, Jr. "Effective Cross Sections for Resonances in HRG," and "Computer Code Abstracts," Technical Activities Quarterly Report, July, August, September, 1966, BNWL-340. Battelle-Northwest, 1966.

DISTRIBUTION

No. of Copies

OFFSITE

1 AEC Chicago Patent Group

G. H. Lee

8 AEC Division of Reactor Development and Technology

Director RDT
Asst. Dir. for Project Management
Chief, Water Reactors Branch (2)
Asst. Dir. for Reactor Technology
Chief, Reactor Physics Branch (2)
D. D. Rauch

1 AEC Division of Reactor Licensing

R. E. Baker

215 AEC Division of Technical Information Extension

3 Argonne National Laboratory

R. Avery
C. H. Bean
R. E. Machery

1 Babcock and Wilcox

H. M. Jones

1 Bhabba Atomic Research Centre

Theoretical Physics Section/RED
Central Complex Bldg.
Trombay, Bombay-85, India

S. R. Dwivedi

1 Brookhaven National Laboratory

J. Chernick

1 Mr. H. B. Brooks
310 Power Bldg.
Chattanooga, Tennessee 37401

No. of Copies

3 Combustion Engineering

W. P. Chernock
R. I-Iarding
S. Visner

1 CNEN - Centro Studi-Nucleaire
Casaccia, Rome, Italy

Ugo Farinelli

3 Edison Electric Institute
750 Third Avenue
New York, N. Y. 10017

John J. Kearney
Harvey Wagner
George Watkins

2 E. I. du Pont deNemours & Co., Inc., SRL

G. Dessauer
H. Honeck

1 ENEL
Via G. B. Martini
(Pizaaz Verdi)
Rome, Italy

Mr. Paoletti Gualandi

3 General Electric Co., San Jose

D. L. Fischer
S. Levy
R. B. Richards

4 General Electric Co., Vallecitos Atomic Lab.

B. F. Judson
T. M. Snyder
R. E. Harris
D. G. Albertson

3 Idaho Nuclear Corporation

E. E. Burdick
R. Grimesey
N. C. Kaufman

No. of Copies

1 Japan Atomic Energy Institute
Tokaimura, Ibarakiken, Japan
Shojiro Matsuura, JPDR-TCA

2 Jersey Nuclear Enterprises
Seattle, Washington
R. L. Dickeman
R. G. Curran

1 Kerr-McGee
Oklahoma City, Oklahoma
Dr. Frank Pittman

1 Massachusetts Institute of Technology
D. D. Lanning

2 Nuclear Materials and Equipment Corp.
C. S. Caldwell
K. Puechl

1 NUKEM
D-645, HANAU
POSTFACH 869
Germany
Mr. W. K. L. Jager

Pakistan Institute of Nuclear Sci. & Tech.
P. O. Nilore
Rawalpindi, Pakistan
M. A. Mannan

1 Philadelphia Electric Company
1000 Chestnut Street
Philadelphia 5, Pa.
Mr. Wayne C. Astley

Power Reactor & Nuclear Fuel Development Corp.
9-13, l-chome, Akasaka,
Minato-ku, Tokyo, Japan
Setsuo Kobayashi

No. of Copies

1 S. C. K. - C. E. N.
MOL-DONK
Belgium

Dr. H. Vanden Broeck
BRL.

2 United Nuclear Corporation

T. B. Holden
J. R. Tomonto

Westinghouse Electric Corporation

R. J. French
R. S. Miller
P. M. Murray
R. E. Olsen
J. B. Roll
J. R. Worden

ONSITE

1 AEC Chicago Patent Group

R. K. Sharp (Richland)

5 RDT Assistant Director for Pacific Northwest Programs

W. E. Fry
P. G. Holsted
J. B. Kitchen
T. A. Nemzek (2)

2 AEC Richland Operations Office

H. A. House
C. L. Robinson

Douglas United Nuclear

C. D. Harrington
C. W. Khulman
W. S. Nechodom
G. F. Owsley
DUN Files (3)

8 WADCO Corporation

J. A. Christensen
E. M. Heck
R. E. Heineman
P. L. Hofmann
L. D. Turner
K. R. Wise
K. L. Young
WADCO Document Control

No. of Copies

88 Battelle-Northwest

F. W. Albaugh
A. L. Bement, Jr.
C. A. Bennett
C. L. Bennett
S. H. Bush
G. J. Busselman
J. L. Carter
N. E. Carter
D. E. Christensen
E. C. Davis (20)
F. G. Dawson
D. R. deHalas
D. E. Deonigi
R. L. Dillon
J. B. Edgar
L. J. Federico
J. R. Fishbaugher
J. C. Fox
M. D. Freshley
G. L. Gelhaus
S. Goldsmith
G. A. Halseth
C. M. Heeb
H. L. Henry
R. M. Hiatt
R. H. Holeman
R. S. Hope
(BNW, Idaho Falls)
U. P. Jenquin
B. M. Johnson
G. J. Konzek
D. A. Kottwitz
J. W. Kutcher
J. H. Lauby
D. C. Lehfeldt
B. R. Leonard
R. C. Liikala
C. W. Lindenmeier
R. P. Matsen
J. L. Maryott
D. F. Newman
D. R. Oden
H. M. Parker
L. T. Pedersen
W. W. Porath
D. L. Prezbindowski
R. H. Purcell
W. L. Purcell
W. D. Richmond
G. D. Seybold
L. C. Schmid
R. I. Smith
W. P. Stinson
G. H. Thomsen
V. O. Uotinen
A. D. Vaughn
R. F. Warnick
R. G. Wheeler
L. D. Williams
N. G. Wittenbrock
W. C. Wolkenhauer
F. R. Zaloudek
M. G. Zimmerman
Technical Information (5)
Technical Publications (2)